CHAPTER 1

FOUNDATION OF THE RESEARCH

1.1 Introduction

The Sundarban region is fringed with the northern Bay of Bengal shores and backed by the prograded Ganga–Brahmaputra Delta, the largest delta in the world (Islam and Gnauck, 2008), over the Bengal Basin. This region supports a vast mangrove ecosystem on the active tidal flats of the region. The only mangrove wetland in the world containing a sizable tiger population, it also supports a dense human population (Naha et al., 2016; Jalais, 2014). The mangrove forests in Sundarban are spread over an area of approximately 10,000 km^2, of which nearly 40% is in India, and the rest is in Bangladesh (Gopal and Chauhan, 2006). The forested area is comprised of protected and open zones. In the open regions, human populace coexist side-by-side the mangrove ecosystem and the animal life dwelling there.

The two districts of the North 24 Parganas and the South 24 Parganas in the Indian state of West Bengal and the three districts of Satkhira, Khulna and Bagerhat of the Khulna Division together contain the Sundarban region (Chaudhuri et al., 1994; Hussain and Acharya, 1994). The South 24 Parganas district contains the majority of the Indian part of Sundarban and almost all of the mangrove forests there. The mangrove region extends from $21^{\circ}31'$ N in the south to $22^{\circ}30'$ N in the north, and from $88^{\circ}10'$ E in the west to $89^{\circ}51'$ E in the east (Ghosh et al., 2002). The western boundary of Sundarban is the Hooghly river, a distributary of the Ganga, and the eastern boundary is the Baleshwari river (also known as the Baleshwar river), which forms a part of the boundary between the Khulna division and the Barishal division of Bangladesh (Rahman et al., 2011b). The Dampier-Hodges line, formulated in 1829–1830 for land management by the contemporary government, is considered the northern boundary of Sundarban (Danda et al., 2011; Hazra et al., 2002). The Dampier-Hodges line roughly matches with a line joining Kakdwip and Bashirhat in West Bengal and then with another line from Bashirhat to Dhaka. The Ichamati river and its distributaries the Kalindi river, the Raimangal river and the Hariabhanga river, which follow the international boundary between India and Bangladesh, form the boundary between the Indian part and the Bangladeshi part of Sundarban (Rahman et al., 2011b).

The accumulation of sediment brought by the Ganga and the Brahmaputra rivers along with numerous smaller rivers and streams flowing in the Ganga–Brahmaputra basin has resulted in the formation of the Sundarban region and the larger Ganga–Brahmaputra delta (Wadia, 1961; Bhattacharya et al., 2012). The delta building process commenced with the arrival of the Holocene and the associated rises in temperature and the mean sea level (Goodbred Jr and

Kuehl, 2000b). The rate of sedimentation was so high that it balanced the rapidly rising sea levels during this period (Goodbred Jr and Kuehl, 2000a). The south-western monsoons have played an influential role in the rate of sediment discharge in this delta, which is reflected in the fact that about 95% of the sediment load carried by the Ganga is delivered during the four monsoon months (Goodbred Jr, 2003).

Within the broad Sundarban, the south-western part of the Indian Sundarban merits special attention chiefly for the following two reasons. Firstly, the geographic environment of the south-western Sundarban has some striking features. Compared to other parts of Sundarban, here the influx of fresh water is low due to upstream sedimentation, which have disconnected almost all the rivers in this region from their original source (Mitra et al., 2009). Most of the inflow of the Hooghly river, the chief source of freshwater in this region in the non-monsoon period, is maintained by the Farakka barrage upstream (Sinha et al., 1996). With the decline in the amount of upstream river water, the flushing capacity of the river stream has decreased. The extensive embankments preclude the carried sediments to be deposited on the banks, leading to riverbed sedimentation (Raha et al., 2012; Ghosh and Mukhopadhyay, 2016). This has lead to both tidal drainage loss of the silted creek and blocking of the channel streams as well as a higher probability of floods (Datta and Deb, 2012). The tidal drainage loss along with higher salinity due to lack of freshwater (Gopal and Chauhan, 2006) has given rise to a more diverse type of topography compared to other areas of Sundarban, which has made this region interesting as an object of academic research.

Secondly, spread of anthropogenic activities within the mangrove zones is considerably higher in this region compared to other parts of Sundarban. In many areas of the south-western Sundarban, human settlements have reached the seashore of the Bay of Bengal (Sarkar et al., 2019). Land reclamation for human activities from inter-tidal zones and estuaries is extensive in this part of Sundarban (Bandyopadhyay et al., 2014). Mangrove resources constitute a major part of economic activities here (Ghosh et al., 2015; Neogi et al., 2016). It is of legitimate academic interest to investigate and study the interplay and effects of this intensive anthropogenic activities on the mangroves. The outcomes of such an investigation may have potential impact on a wide and vast mangrove ecology and a large number of human occupants of this region.

The objective of the current research is investigating the geo-environmental settings of two islands in the south-western Sundarban, with striking and varied features justifying their selection as study areas. These two islands are accessible to all seasons (pre-monsoon, monsoon and

post-monsoon) to carry out the research described in the following sections. Most of the research is based on primary data collected from direct field measurements on soil characteristics, mangroves, geomorphic and hydrological features. No such extensive work has been carried out in these region before in such local scale with consideration of settings and sub-settings of the island physiography.

The diverse geomorphic settings of the south-western Sundarban region include tidal flats, mudflats, salt marshes, swamps, tidal creeks, salt encrusted regions, etc. In fact, the relatively small area of south-western Sundarban contains all the geomorphic settings that can be observed in the broader Sundarban mangrove region (Ganguly et al., 2006). The geomorphic settings influence the characteristics of the local ecosystems (Woodroffe et al., 1992), which vary from dense mangrove forests in the swamps to perched and almost barren tracts in the saltpan regions. In the estuaries, tidal flats are prominent, which influence mangrove proliferation and succession (Qiaomin et al., 1997). Salt marshes develop in the middle and upper parts of the tidal flats, and contain mangrove grasses and herbaceous mangrove plants (Sengupta and Chaudhuri, 1990). In pockets of the regions with lower levels of water availability, saltpans emerge from evaporative salinity build up in the soil, which also degrades the existing mangrove habitat there (Chakravortty and Ghosh, 2018). The numerous tidal channels in the estuarine regions transport tidal water as well as sediment to the interior of the region.

The coastal processes of the Bay of Bengal influence the regional physiography of the region. The ongoing climate change affects the dynamic but fragile mangrove habitats (Field, 1995). The rising sea level threatens the mangrove habitat with submergence (Hazra et al., 2002), while the increasing frequency of cyclones brings widespread devastation (Ali et al., 2020). The high load of sediments brought by the Ganga–Brahmaputra river system are deposited on the estuary bed, which causes the emergence of new islands over time. Often, the islands becomes connected and part of the mainland due to further siltation. The south-western Sundarban has both open coastline and semi-sheltered estuarine region (Ghosh and Mukhopadhyay, 2016), and hence affected by both the estuarine processes and tidal processes in an open coast. For the dwelling populace in this region, the coastal climatic hazards like storms and floods are very much a cause of concern, especially because these occur seasonally every year (Madsen and Jakobsen, 2004; Balaguru et al., 2014). The topography and physiography of this region has been extensively altered by the dense human population residing there (Ghosh et al., 2015). Though the extensive artificial embankments constructed here obstructs tides and storm surges

from entering the agricultural and aquacultural fields and dwelling places, they also disrupts the natural hydrology of the region and degrades the mangrove habitats (Dhara and Paul, 2016; Ghosh and Mistri, 2020b). The shoreline of the region changes due to erosion, accretion and human influence (Ghosh and Mukhopadhyay, 2016; Jana et al., 2017).

The different geomorphic settings of the region affects the soil and water characteristics (Daniels and Hammer, 1992). The soil texture and its composition in sand, silt and clay varies considerably within the settings. The chemical components of soil and the salinity of water vary significantly among the geomorphic settings (Pinay et al., 2000). The saline blanks, which are observable in many places in the south-western Sundarban, emerge due to excess salt deposition on the soil surface and negatively affect the mangroves (Selvam et al., 2012). The mangroves in turn vary considerably with the topographic settings (Sreelekshmi et al., 2020). A major part of the region undergo periodic inundation during high tides, and this affects the mangrove vegetation in this region (Rogers and Goodbred, 2014). The larger storm surges and the cyclones create overwash deposits, which bury and destroy the existing the mangroves in the shore (Paul et al., 2017). On the other hand, they also provides a pressure towards the landward migration of the mangroves. Bioturbation by organisms dwelling on the coast leaves a significant impact coastal environment, including soil nutrient and texture, and the shoreface (Das et al., 2012; Sen and Homechaudhuri, 2018). In the estuarine region, saltmarshes and mangrove swamps influence and alter the geomorphic characters of the region over time (Coleman et al., 2021).

The rainfall in this region is concentrated in the monsoon season and is the chief source of freshwater (Chakraborty and Mandai, 2008). However, it is of import to investigate the changing rainfall characteristics over time in the face of ongoing climate change (Sahana et al., 2020). Similarly, temperature characteristics are also affected by climate change (Dubey et al., 2017; Gopal and Chauhan, 2006; Neogi et al., 2016), and along with temperature and rainfall, relative humidity levels are affected. The evapotranspiration rate increases with rising temperature, further straining the water availability. With changing climate, the mangrove characteristics like density and forest cover also changes (Neogi et al., 2016). The biomass of mangroves varies with changing mangrove properties (Akhand et al., 2017). The strained water budget along with the water requirements of the human population is met by groundwater extraction (Bhadra et al., 2018). However, groundwater exploitation may not be sustainable (Gayen and Zaman, 2013). The drainage of the region is determined by the numerous creeks and channels criss-crossing this region, many of which have suffered from tidal drainage loss due to blocking

of channels by siltation and human activity (Ghosh and Mistri, 2020a,b). In view of the strained water availability, it is of import to have a proper assessment of the water budget in this region.

The coastal environment is fragile, and in the face of climate change related threats, it is of import to device and implement proper management plans and techniques of the coastal resources (Rahman et al., 2010). A large population depends on the coastal resources for their livelihood, and to ensure the economic security of the local populace, implementing a sustainable management plan in this region is necessary. In the Sundarban mangrove region, management and restoration of the mangrove forests is of primary import (Das and Mandal, 2016), as the mangrove habitat is the pillar on which most of the other aspects of the coastal resources rest on. Salt encrustation of the soil surface and the resulting saltpans leads to local deforestation of mangroves. So, it is required to manage the formation of saltpans in the mangrove areas, and if possible, to reverse it. Fishing and related activities is a major source of employment in this region (Ray, 1993; Haque, 2003), and its sustainable management is required. Sustainable ecotourism development in this may be an avenue that would guarantee both the economic security of the populace and the flourishing of the natural ecology (Khanom et al., 2011; Das and Bandyopadhyay, 2013). However, any management plan needs to take care of the increasing stress on the livelihood and possible ways of adaptation (Mistri, 2013).

For the close investigation of the above features, two islands in the south-western Sundarban are selected. The locations of the two islands and the justifications for their selection are described in Section 1.2. In Chapter 2, the geomorphic settings in the study area are described in detain along with the elevation contours. The ecosystem functions of the geomorphic settings, and the formation and evolution of those settings are also described along with appropriate cross profiles. The coastal environment of the study area and its transformations in the face of climate change along with human influences are discussed in Chapter 3. The physiographic settings of the islands and their environmental assessment, including soil and water characteristics, aspects of tidal inundation and the bioturbation process are presented in Chapter 4. The variation in the mangrove characteristics, impact of the overwash process and the changes in the shoreface environment are also presented there. In Chapter 5, the temporal analysis of rainfall, temperature, relative humidity and evapotranspiration rate are presented. The relationship of the climate variables with the mangrove density and the implications of the temporal trends of the climate variables on the mangroves are also presented here. The groundwater consumption trend and its sustainability are also discussed. The available water budget in the islands are detailed.

Plans for coastal resource management including forestry, fisheries, livestock are ecotourism development are described in Chapter 6. After that, the major findings are summarized, and recommendations are given for the conservation of the existing ecology in the face of the changing climate.

1.2 Location and significance of the study area

The study area of this research work consists of two islands in the south-western Sundarban: the Patibania island and the Henry's island, and their surrounding areas. The islands are located in the region of the south-western Sundarban bounded by the Muriganga and the Saptamukhi rivers, and are adjacent to Bakkhali. Although the islands are located very close to each other, with less than 3 km distance between them, there are striking differences in their geomorphological and ecological characters. The Patibania island is a reserve forest and hence almost free from human activities and the resultant impacts on the topography and the ecology of the island. On the other hand, there is no such restriction in the Henry's island, and consequently, its topography and ecology are shaped by agricultural and aquacultural activities carried out in the island and also by tourism enterprises.

In Figure 1.1, the locations of the study area containing the Henry's island and the Patibania island in the Indian state of West Bengal is depicted. The position of the two islands in the south-western Sundarban region is presented in Figure 1.2. Maps of the Henry's island and the Patibania island are presented in Figure 1.4 and Figure 1.3, respectively.

The Patibania island is part of the larger Mousuni island. The latitudinal extent of the Patibania island is from $21^{\circ}36'38''$N to $21^{\circ}34'39''$N, and the longitudinal extent is from $88^{\circ}15'30''$E to $88^{\circ}14'21''$E. Bounded by the Muriganga river on the west and the Edward's creek on the east and the south, the island has humid sub-tropical climate with high monsoonal precipitation and a dry season between November and April. The average temperature there is around 26°C and the average yearly rainfall is around 1500 mm–1600 mm. Most of the yearly rainfall occurs in the monsoon season, and a low amount of rainfall occurs in the post-monsoon season.

The Henry's island is located on the shore of the Bay of Bengal beside the Saptamukhi river estuary. The latitudinal extent and the longitudinal extents of the Henry's island is from $21^{\circ}35'40''$N to $21^{\circ}33'31''$N and $88^{\circ}18'19''$E to $88^{\circ}15'44''$E, respectively. The island is a popular destination for mangrove ecotourism. In addition, aquaculture and fish processing and drying are

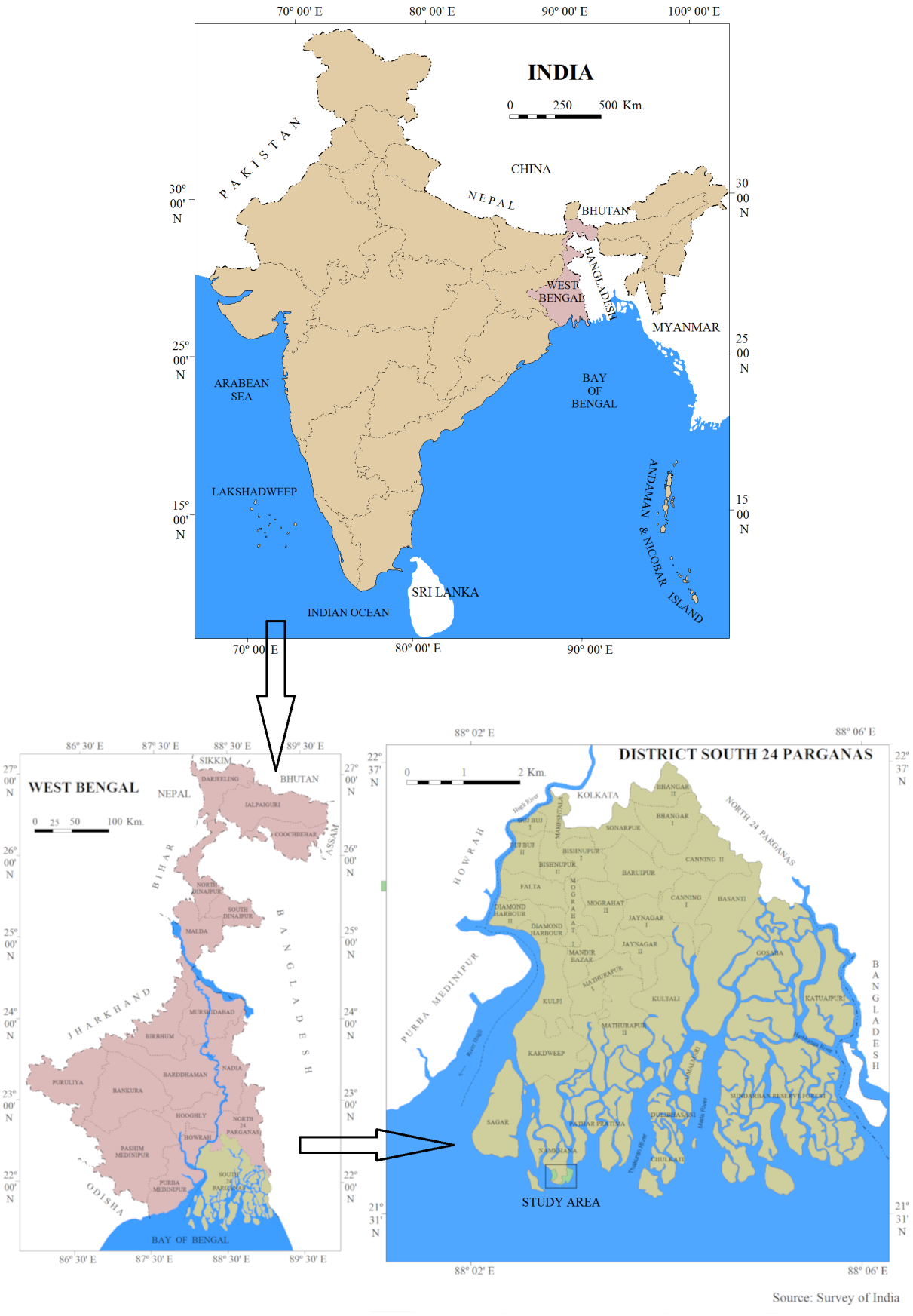

Figure 1.1: Location of south-western Sundarban in West Bengal, India.

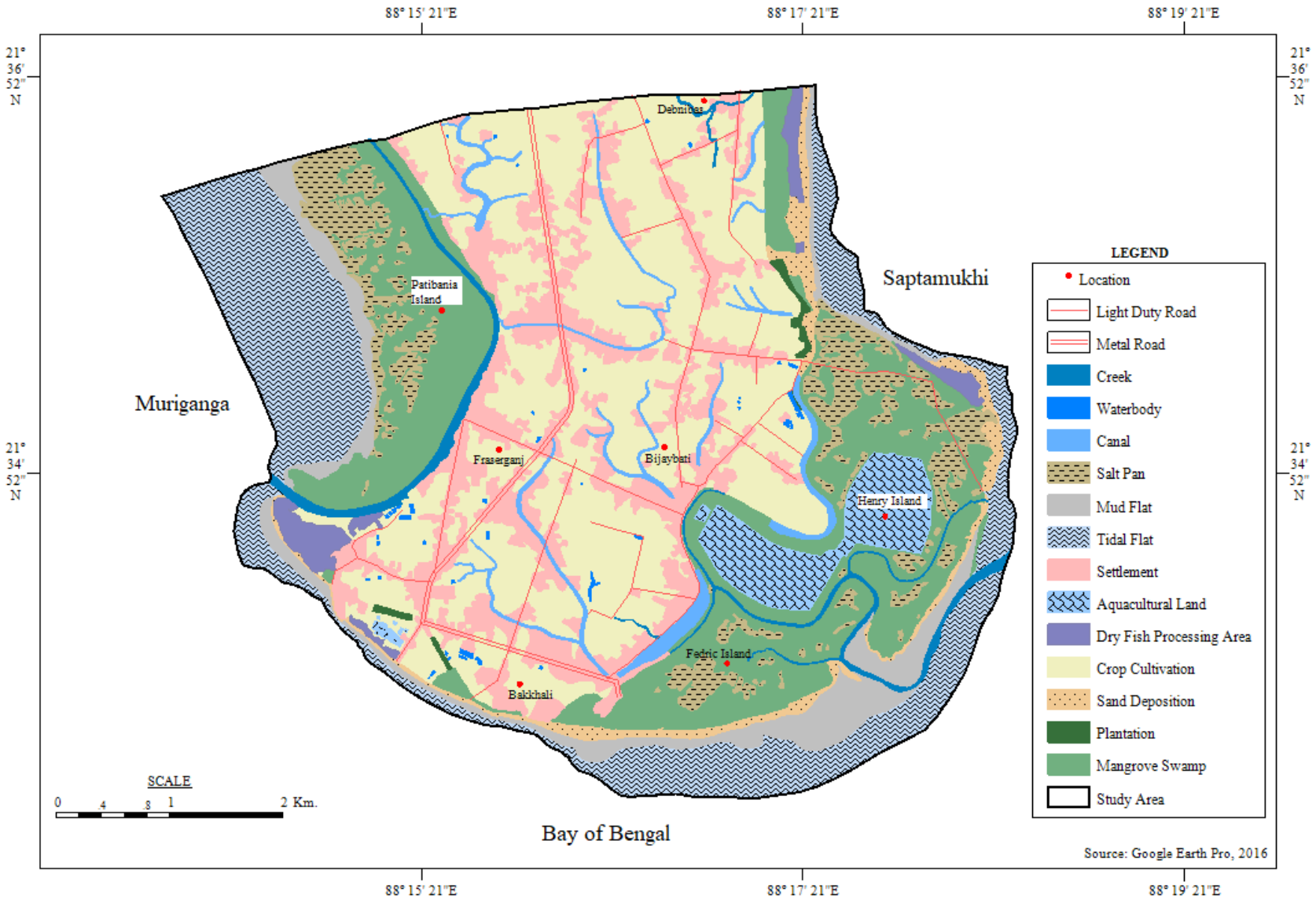

Figure 1.2: Position of the Patibania island and the Henry's island within south-western Sundarban surrounded by the Muriganga estuary and the Saptamukhi estuary.

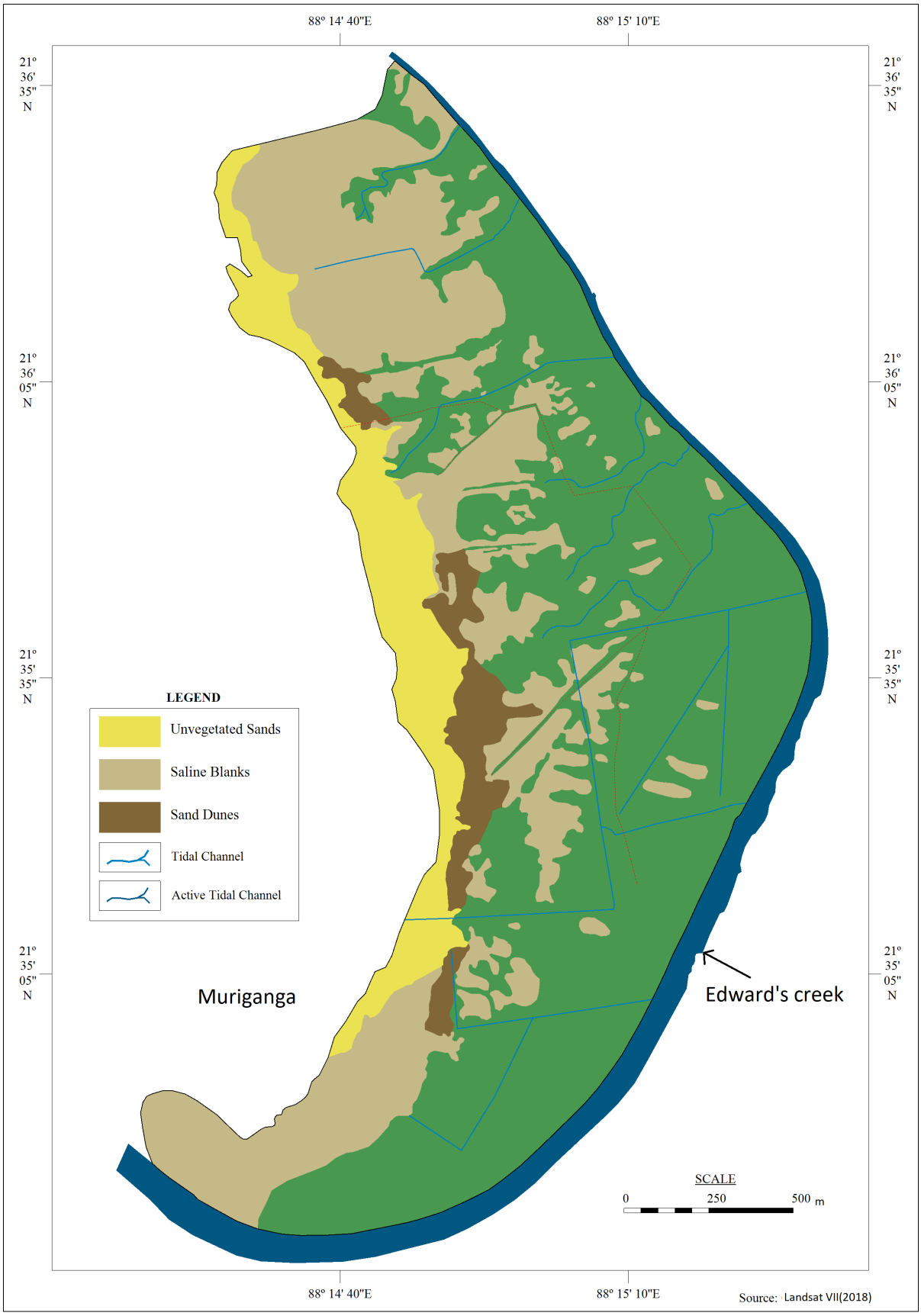

Figure 1.3: Map of the Patibania island.

Figure 1.4: Map of the Henry's island.

other significant economic activities carried out in the island. Bounded by the Saptamukhi river in the east, the Bakkhali creek in the west and the Bay of Bengal in the south, the Henry's island has distinctive geomorphological features and mature development of hypersaline patches. The climate in the Henry's island is identical to that of the Patibania island.

Among the notable geomorphological features in the Patibania island, there are bare sand feet, active tidal channel, abandoned tidal channel and mangrove swamp. The slope of the island is from the eastern to the western parts. There is a tidal flat in the eastern section of the island with elevation 4 m, whereas a depression has formed in the middle part with elevation 2.5 m. The western part of the island has elevation 1.5 m to 1.7 m. Due to this topographic setting, normal monsoonal tides that breaches the bank margin ridge and reach up

to 4.5 m leave saline water trapped in the middle part of the island at least for a few days. The evaporation of this stagnant tidal water results in deposition of salt in the soil, which has caused the formation of salt patches in this part of the island. The regions with elevation below 4.5 m are frequently inundated during high tide, which results in seasonal changes in the characters of the the salt patches. Likewise, the distribution and the variation of the mangrove species also undergo seasonal changes. Tidal drainage loss is an active process throughout the island, and it influences the topography and the ecology of the island.

One notable aspect of the ecology of the Patibania island is its mangrove zonation and pattern, which is strikingly different in comparison to the other islands of Sundarban. Mangroves are dwarfed in the older tidal flat of the island where salt patches are abundant. Number of mangrove species in the area dominated by salt patches are comparatively low, whereas the diversity of mangrove species is maximum in the eastern part of the island on the active tidal flat adjacent to the tidal creek. The influence of the geomorphological features on the local mangrove ecology is thus clearly distinguishable in this island.

The area in the Henry's island can be classified as a coastal plain estuary. Notable land forms present in the island are mangrove swamp, mudflats, salt flats, hyper saline patches, creeks, salt ponds, over wash fan lobes, etc. The tidal mudflats provide a favorable environment for the development mangrove species and subsequent colonization by mangroves. Some tidal flats in the island have planated mud banks. The salt flat have relatively thinner vegetation cover due to its hypersaline environment, which is adverse to the proliferation of greenery. The coastal processes active in this area which play influential roles in shaping the topography and the ecology include sedimentary deposition, tidal drainage loss, shoreline erosion and development of hypersaline tracts within mangrove covered zones. Micro-topographic features of the surface traps both saline water from storm surges and tides and fresh water from monsoonal rainfall, which assist in the expansion of wetlands towards the inner parts of the island. Development of saline patches within mangrove swamps are notable in the Henry's island. Blocking of tidal creeks, hypersaline conditions and topographic depressions are major reasons behind the development of saline patches. The physiographic settings in the island shaped by human undertakings include mangrove restoration tracks, planted vegetation on the tidal flats and aquaculture ponds in the central part of the island.

The mangroves in the Henry's island vary in their density and diversity both spatially and seasonally. The spatial variation is determined by the soil characteristics, the geomorphic

settings, tidal inundations and storm surges in the shore and the creek banks and human activities. Seasonal variation of mangrove distributions is caused by monsoonal rainfall and the consequent changes in pore water salinity and the hot and humid conditions of the climate. The climatic variations due to the monsoon and the relatively dryer conditions for the rest of the year also cause seasonal changes in the soil character, which in turn affect the mangroves. The densest mangrove forests are seen along the shoreline due to plantation of coastal vegetation to protect from natural calamities. Density of the mangroves decreases in the inland areas largely owing to human activities.

Large areas of mangrove forest in the Henry's island are degraded due to human economic activities and settlement since 1970's. Over exploitation of mangroves and expansion of tourism and aquacultural activities have resulted in substantial reduction in the mangrove covered region. Climate change and geomorphological processes also have played their parts in the degradation of mangroves. Increasing temperature, high evaporation rates, sea level rise, high intensity of cyclones and frequent coastal flooding have caused adverse changes in the abundance patterns of the mangrove species in the Henry's island. Also, tidal drainage loss and overwash sand deposits in the inner parts of the shore from erosion have negatively affected the mangrove distribution. Cumulative effects of changing weather patterns, subsidence of low lying areas, increase in salinity and development of salt patches within mangrove swamps create an imbalance of fresh water and saline water in the island, retard the growth of mangroves.

The Henry's island and the Patibania island are selected because of their distinctive features and significant differences among them. Henry's island is situated at the Saptamukhi river estuary, where the influx of freshwater is negligible because all the channels and creeks are disconnected from their original source. However, the Patibania island is located at the Muriganga river estuary, where fresh water influx is higher because the Muriganga river is connected to the Hooghly river through active tidal channels. The Henry's island is a reclaimed island popular for its ecotourism complex and fishing project and Patibania is a reserve forest area protected by the forest department. This makes the Henry's island suitable to study the mangrove ecology and its spatial and temporal variation in the presence of anthropogenic influences, while the Patibania island is an ideal place for investigating the diversity in mangrove ecology with the variation in geomorphic settings and climatic fluctuations. Mangrove sensitivities to the climate change also vary in the two islands with changing physiographic settings.

1.3 Modern coastal process

The coastal landforms are shaped by several factors including waves, tides, winds, storms, and also the mean sea level (Wright and Thom, 1977; Masselink et al., 2014). The physiography and ecology of the Henry's island has changed significantly under the influence of the coastal processes. The swampy intertidal zone and some parts of the backshore of the coast of the Henry's island, which were above water in 1969, have now been submerged. Topographic character, shoreline change, ingress of the sea, modern sands, transported from near coastal seabed are deposited on the ancient clayey silt bed depending on retreated by 450 m to 1 km. Polen of Liliceae, Pteris, Microthyroid, Excoecariaan, Rhizophora in the subsurface sediments indicate the swampy nature of the earlier coast.

The coastal processes can be divided in three broad categories, which are physical processes, hydrological processes and biological processes.

1.3.1 Physical process

The principal drivers of the physiographic changes in a coastal region are waves and tides. Saptamukhi river and Bakkhali river both are considered as tidal creeks but do not discharge considerable amount of freshwater and sediments. The present intertidal zone is converted into mangrove vegetated backshore. In general the width of the intertidal zone varies from 36 to 450 m. In the central sector of the beach, the the width is as narrow as 36 m and sand spit to connected main coastline beach around 450 m in generally, slope of the beach ranges from 0.13° to 4.2°.The widest part of the beach has very gentle slope (0.13°) and the narrowest part of the beach which is in the central part, shows steeper slope (2.53° to 4.2°). On the foreshore region, backwash ripples and cross ripple marks are observed along with long shore bar and runnel (Saha et al., 2014). The backwash of the waves, which creates a turbulent motion on the fine sands, creates the backwash ripples. There are clay balls in some sectors of the intertidal zone (around $21^{\circ}34'27.9"$N, $88^{\circ}17'58.4"$E and $21^{\circ}34'31.9"$N, $88\circ18'0.4"$E). These clay balls have been transported by the waves from a submerged erosion-prone zone in the near-coastal water.

The foreshore has a mature sand dune belt of about 20–160 m width along the coast. The high water line is at the base of the dunes. The sand dunes, as a result of natural processes, are flattened at places and the relief ranges From 3 to 4.63 m. During high tides, the maximum

water level sometimes crosses 4 m. However, tidal water is not observed to inundate or reach the upper parts of the sand dunes (Saha et al., 2014). Low relief neo-dune belt of about 40 m Width has been developed in the western sector. Some small shoals have developed at the confluence of the Saptamukhi river.

During the present course of study it has been seen that the island system of the Hoogly-Matla estuary is suffering a significant amount of net land loss in spite of the reactivated delta progradational process. Significant beach lowering has been observed over the erosional domains of the coastal tract (Hazra et al., 2002). A steady rise in the annual mean sea level is observed between 1985 and 1998, which has accumulated to a minimum of 4 cm rise in the relative sea level (Hazra et al., 2002). A yearly rise of annual mean sea level has been estimated to be 3.24 mm per year, which is considerably higher than the current trend of average global sea level rise at 2 mm per year (Nautiyal et al., 2016). From the present relative sea level rise at 3.14 mm per year, it can be estimated that the compound sea level rise would become close to the 1 m scenario of (Broadus, 1993) by the year 2050. The estimated rise of sea level will create serious threats particularly during the pre- and post-monsoon period when most of the cyclonic storms occur in the Bay of Bengal.

1.3.2 Hydrological process

In the Indian Sundarban, the most significant and influential estuaries are of the Hoogly river and the Matla river. Apart from these two, the other big estuaries are Saptamukhi, Thankuran, Bidya, Goasaba and Raimongal. In addition, there are innumerable big and small rivers criss-crossing Sundarbans. Many rivers have completely lost their upstream freshwater sources due to siltation and have become tidal creeks (Sanyal and Bal, 1986). Except Hooghly and Raimongal, none of these estuaries are having freshwater flow. These estuaries are more than 70 km in length starting from its head to the meeting point at the Bay of Bengal. A major part of these estuaries pass through inhabited regions, and an inflow of nutrients occur from these regions in the form of agricultural field wash and aquaculture pond effluents. However, mangrove detritus is relatively scarce in the rivers.

The hydrological behavior of Sundarban is determined by freshwater flow from the upstream, tidal flow from the river mouth, currents and waves, topography of the ecosystem (Wahid et al., 2007). The drainage network in Sundarban in constituted of inter-connected estuarine rivers and cross channels. Climate change and occurrence of cyclones over Bay of Bengal, tidal

regime, sub surface flow, sheet flow, and monsoonal water controlled the hydrological character of Sundarban. During the May to October tidal inundation regulates the hydrology of the area of Sundarban Area inundation - by normal high tides , areas inundated only -by spring high tides, areas inundated -by the high monsoon tides, area inundation by all tides: The mouth of big rivers and along the sea coast.

In recent years, groundwater in the delta has been the subject of attention because of water quality issues. The monsoonal rainfall strongly influences the groundwater flow. The annual rainfall in Sundarban ranges from about 1200–1600 mm (Wahid et al., 2007). The soil and water salinity in Sundarban depends on the volume of freshwater inflow from upstream flow of the Ganga river and the monsoonal rainfall. The daily highest salinity level is usually reached with the peak tidal height on that day. The daily range of salinity level also undergoes seasonal fluctuations. The Henry's island and the Patibania island are criss-crossed by intricate network of creek system. Henry's island is located near Saptamukhi river estuary. It has its origin at Sultanpur. The Saptamukhi river is connected with the Muriganga river through the Hatania-Duania canal (Mitra et al., 2009). On the other hand, the Patibania reserve forest is located at the Muriganga river estuary, which is a branch of the Hooghly River. In terms of availability of fresh water, Muriganga is providing much fresh water to the Patibania island through the creeks and canals. But availability of fresh water is negligible in the Henry's island.

1.3.3 Biological process

The organic matter content on the mangrove regions act as an important nursery ground for many commercially important fish species. Due to large scale human intervention from the beginning of last century, several species have become extinct or are in very much threatened or degraded state Gopal and Chauhan (2006); Sodhi et al. (2013), Eutrophication seems to be a global problem and nutrient enrichment is one of the most serious threats to near shore coastal ecosystems (Cloern, 2001). The balance of a water ecosystem is disturbed by eutrophication. The extra nutrients leads to increase in phytoplankton quantity and algal blooms. Estuaries receive considerable amounts of dissolved and particulate organic matter and contaminants from land. Estuaries also receive nutrients and organic matter loads from wetlands such as marshes (Meybeck, 1982).

1.4 General topographic description of the islands

The Henry's island and the Patibania island are part of the Saptamukhi–Muriganga estuarine system, and their topographies are shaped by the estuarine processes and tidal and wave action. The notable topographic features in the two islands include sea beaches, tidal shoals, sand dunes, tidal flats, mudflats and mud banks, salt marshes, swamps, The layout of the Patibania island is in the north–south direction with an inward curved coast. Its southern end has a sandy beach and it protrudes out into the confluence of the Muriganga river with the Bay of Bengal. Its western coast has a narrow beach with the occasional tidal shoals. The eastern boundary has an elevated bank margin ridge along the Edward's creek. Behind the beach, there are on it. The Patibania island is Numerous channels and tidal creeks have dissected the land mass of this estuarine system into many smaller islands. Almost all of the channels have lost connection to their upstream sources due to sediment build up. Deposition of modern sands over the ancient clayey silt sediment is in the process of transforming the swampy intertidal zone into a sandy beach in this region. Topographic characters of the two islands influence the spatial distribution of vegetation cover and development of saline blanks.

To identify the general topography of the islands, Cartosat 2A DEM is used. The digital elevation models of the two islands are presented in Figure 1.5 and Figure 1.6.

The digital elevation model of the Henry's island reflects its general slope, which is from the west to the east. Highest elevation (2.40 m) is found along the shoreline due to the location of sand dunes. Central part of the island has elevation of 1.20 m, while the general topographic elevation of this island is 1.50 m. The relief of the Henry's island plays a significant role in the drainage network system and the distribution of mangroves. Topography and surface character of the Henry's island reveal the presence of several depressions, within which saline water gets accumulated during tidal inundation. In due course of time, this water gets evaporated leaving the salt content on the ground. The salt thus accumulated encrusts the surface of these depressions and form hypersaline patches over time. Detailed description of the contour plan of these saline blanks and the micro-zonation of the island are discussed in Chapter 2. The characteristics of the vegetation in the Henry's island are described in Section 1.5.

The elevation of majority of the areas in the Patibania island is between 1.78 to 2.38 m. Highest elevation is observed in the western part of the island (2.90 m) along the overwash lobes. Eastern part, which has a bank margin ridge, has moderately high elevation. In Figure 1.7, the elevation along a cross section traversing from the west to the east in the middle part of the

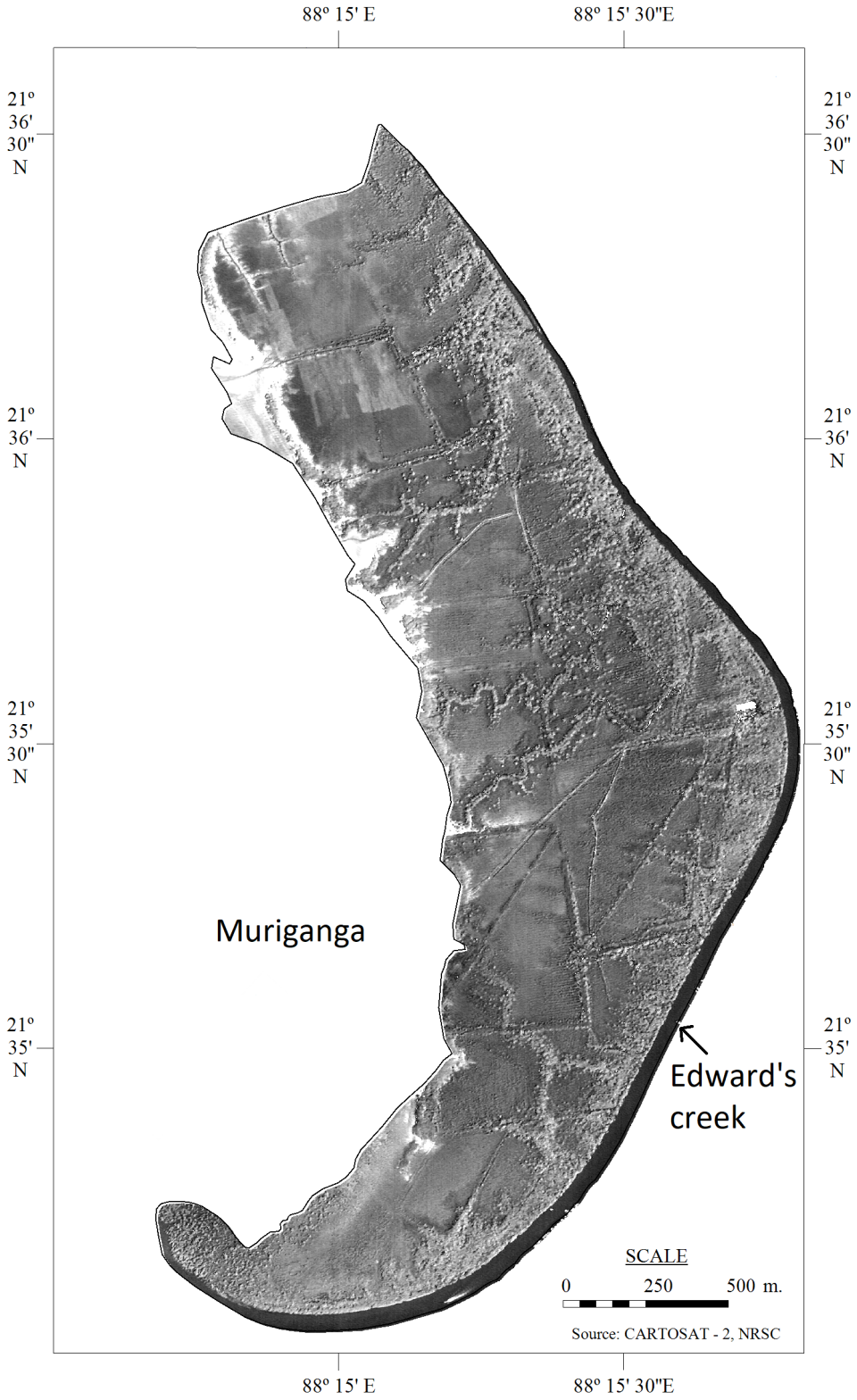

Figure 1.5: Digital elevation model of the Patibania island.

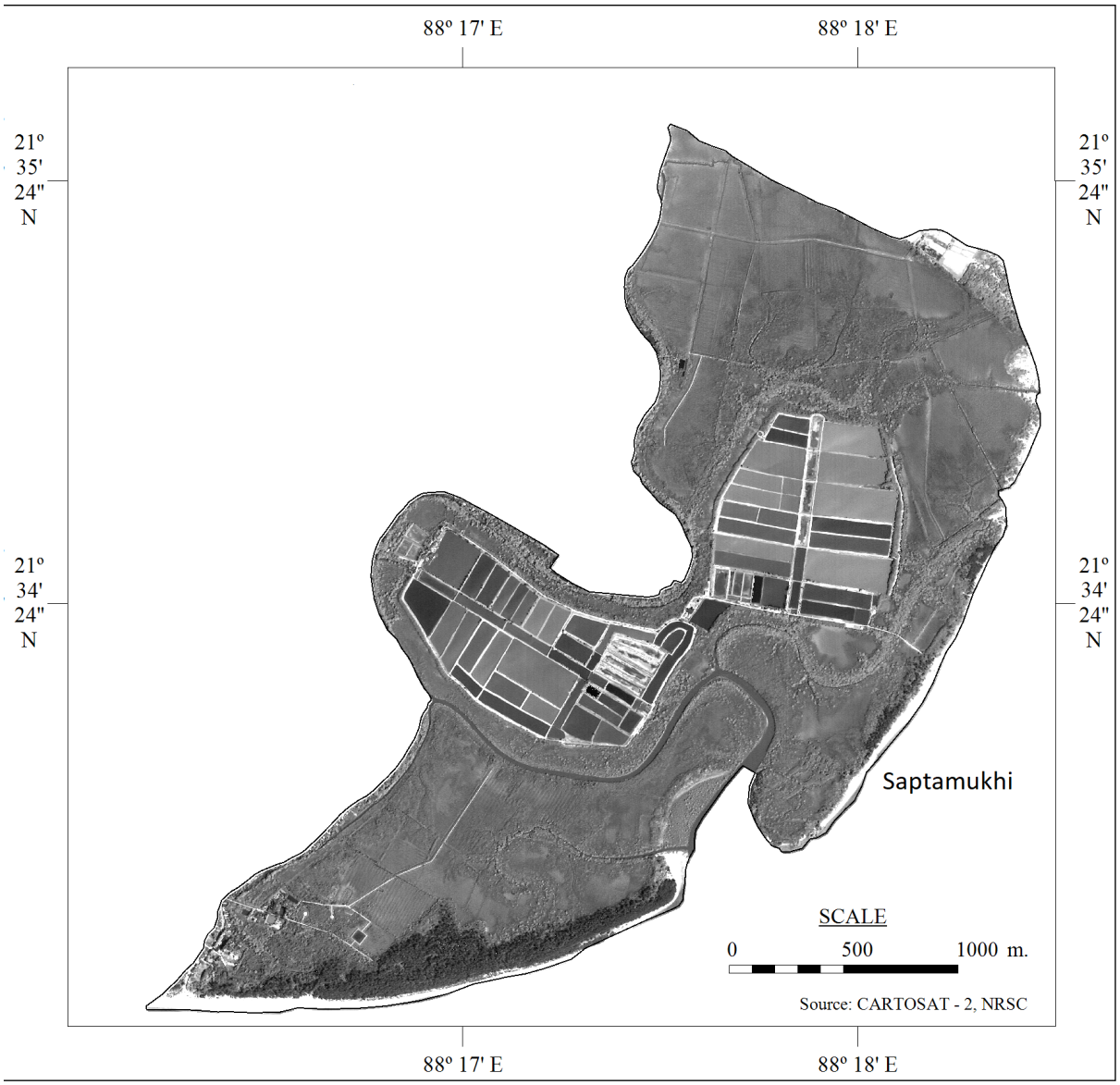

Figure 1.6: Digital elevation model of the Henry's island.

island is presented. From this elevation profile, it can be seen that the middle-western part of the island has lower elevation compared to the eastern and the western parts, and it forms a basinal shape. This shape is responsible for the development of saline blanks here and typical mangrove features throughout the island. This depression gets inundated with saline water after spring tides and high storm surges, and subsequently, saline patches develop here from evaporative deposition of salt. Detailed description of mangrove characters and its spatio-temporal changes in the Patibania island is presented in Section 1.5.

From the field study, it was observed that there is a close relationship between the distribution of mangroves and the elevation in the Patibania island. On the basis of the mangrove

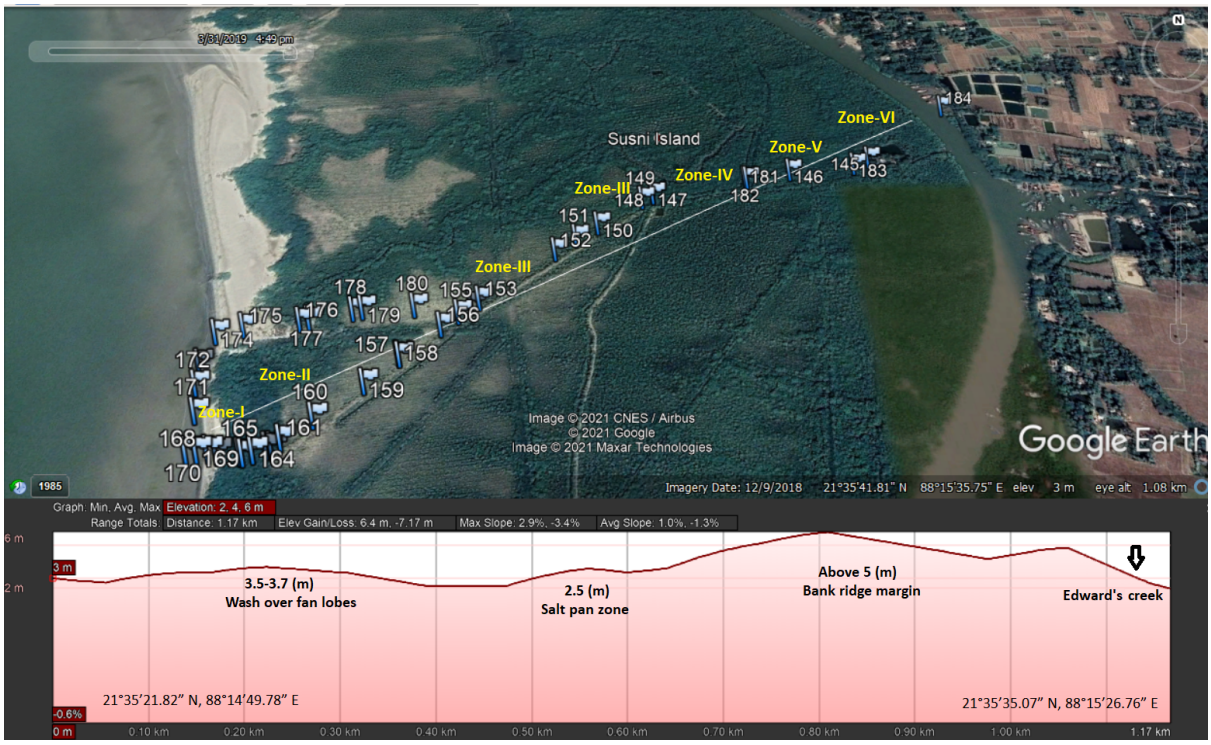

Figure 1.7: Cross section showing the general surface profile of the island.

characteristics and the elevation, the island area can be divided in six zones from the west to the east. In Figure 1.7, the locations of the zones are depicted in a cross profile drawn from the west to the east. The features of the zones are described below.

Zone 1: A tidal shoal is observed at the elevation of 1.5–1.7 m from the mean sea level on the western fringe of Patibania island. A linear sand bar is located from the north to the south on the same surface parallel to the shore line, which is formed by wave deposition of sandy materials. A wide and extensive mudflat has formed in this zone with accumulated fresh silts and sticky clay materials with evaporated surface and frequent tidal exposures in the low tide. On the other hand, the island fringe tidal flat is frequently inundated during high tides.

Zone 2: In this zone, the shore fringe sandy beach is located at the high tide line, which is formed by washover sands, and it has elevation of 3 m. Also, there are several marks of different high tide lines at different lunar phases with litter zones over the sandy beach. The sloping beach face of sandy materials are reworked with aeolian activities at the drier marks. As this shore fringe surface is very narrow on the western fringe of the Patibania island, it is unable to hold the advancing sea waves during high tides at the time of equinoxial tides, storms and cyclones. Wide areas of overwash sand fan lobes are extended from these zones towards the island interior. The higher and wider sand fan terrace lobe surface is colonized by rich forest in

this region.

Zone 3: This part of the island is lower than the shore fringe beaches at the elevation of 2.5 m. This area extends along a wide front with an width over 100 m from the landward end point of the shore fringe to the inland part of the island. Also, there are numerous hypersaline tracts with stunted growth of mangroves shrubs in this zone. The hypersaline regions are rarely flooded by high tide water in this part of the island. Only during the monsoon season, these regions are flooded for around two months during the year. This zone also has a compact muddy terrain with a thin cover of wind-blown sand particles and salt encrusted surface. The soil moisture of this terrain remains very low in the non-monsoon period with desiccated mud cracks.

Zone 4: This zone of the Patibania island is colonized by mangroves trees of moderate growth and good foliage. There are also some dry and wet salt ponds in between colonies of vegetation. Extensive pneumatophores are distributed over the open surface in this zone that can accumulate sediment and organic matter during the high tides. This zone has elevation of 2.2–2.4 m, and it is frequently inundated during high tides, particularly during the south-western monsoon months (June–October). The soil moisture of this zone is slightly higher in compare to the previous zones of the Patibania island. In addition, this zone has moderately soft muddy surface, and there are relatively fewer saltpans and evaporated muddy patches. The width of this zone is over 300 m.

Zone 5: This zone of the island contains a nutrient rich tidal flat with high soil moisture and moderately luxuriant growth of mangroves. The elevation of this zone of the island is over 3 m towards the Edward's creek. The width of this zone is about 500 m from the boundary of the previous zone to the Edward's creek. A pond is located here filled with brackish water that is availed by the animals of this island for drinking. The mangrove floor of this zone is colonized by under growths and thick deposition of dry and wet biomass over the soil surface. The soil moisture of this zone is relatively high compared to the previous zones.

Zone 6: This zone situated on the eastern fringe of the island with a bank margin ridge is the most attractive zone for mangroves. This part of the island is composed of soft mud and drained by several tidal creeks. This zone is fringed with extensive bare mud flats on the eastern side with knee deep mud on the creek bank. The soil moisture of this zone is very high in comparison to the previous zones of the islands due to frequent tidal inundation and natural infiltration of saline water and freshwater. Due to this, this zone is the richest in biodiversity

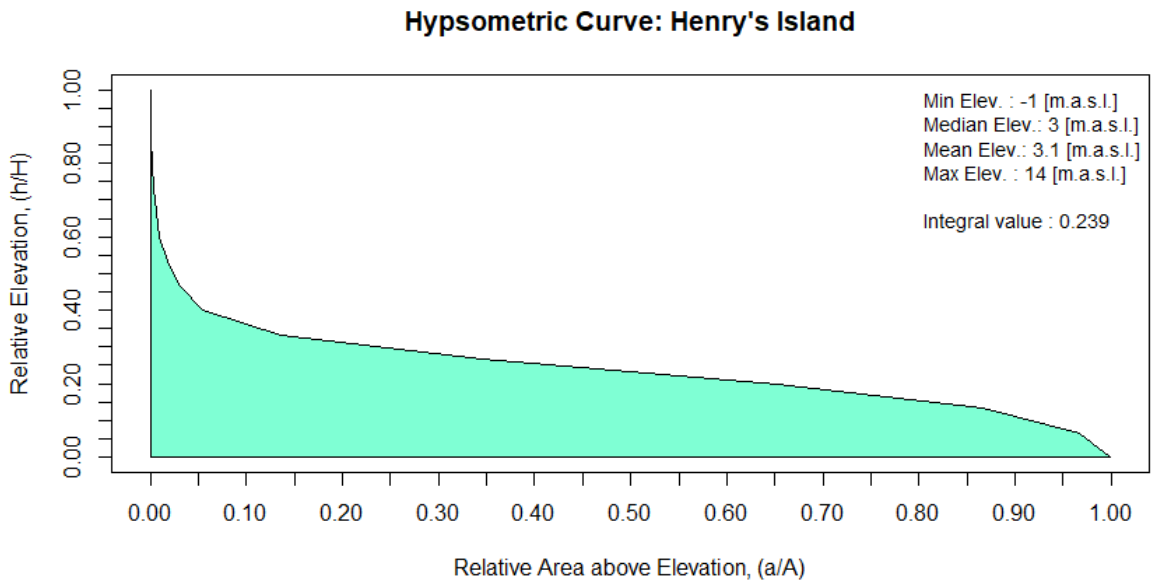

Figure 1.8: Hypsometric curve of the Henry's island.

within the island. The elevation of this zone is above 5 m.

To assess the geomorphic maturity of the islands, hypsometric metric curves of the islands are drawn. The hypsometric curve of a geographical area is obtained by plotting the relative elevation in that area against the relative area above that particular elevation. The hypsometric integral is the area bounded by the hypsometric curve and the two axes, and its value is an indicator of the stage in which that area belongs in the cycle of erosion (Strahler, 1952; Singh et al., 2008). There are three stages in the cycle of erosion, which are old, mature and young. The value of the hypsometric integral is less than or equal to 0.3 for the old stage, it is more than 0.3 but less than or equal to 0.6 for the mature stage, and for the young stage, it is greater than 0.6 (Strahler, 1952; Singh et al., 2008). In Figure 1.8, the hypsometric curve of the Henry's island is presented, and the hypsometric curve for the Patibania island is depicted in Figure 1.9.

The hypsometric integral values for the Henry's island and the Patibania island are 0.239 and 0.368, respectively. From these values, it can be concluded that the Henry's island is in the old stage of the cycle of erosion while the Patibania island is in the mature stage of the cycle of erosion.

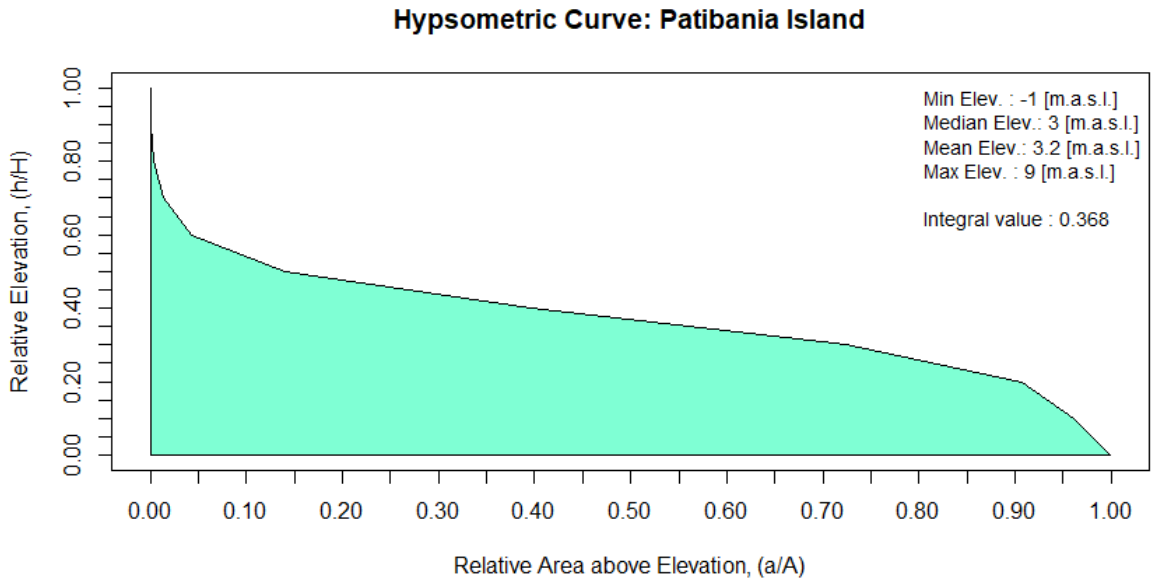

Figure 1.9: Hypsometric curve of the Patibania island.

1.5 Spatio-temporal variation of vegetation

There is a close relationship between topography and mangrove characters in a region. The spatial distribution of mangroves is determined by fresh water influx and saline water intrusion along with topography. The topography also plays a significant part in determining the locations and quantities of saline water intrusion in the island through tidal inundation. Daily tidal inundation normally only inundate the low lying areas adjacent to the sea or the creeks. But inundation due to storm surges and spring tides submerge the island even exceeding an elevation of 2 m. So, the low lying areas on the seashore and the creek banks get inundated frequently, which significantly hampers vegetation succession. But the high elevated areas are seldom submerged, and hence are more suitable for dense mangrove growth. During storm surges and spring tides, saltwater sometimes breaches or overflows the dunes in the Henry's island and inundate the low lying areas behind them. This causes a negative impact on the mangrove succession in those depressions through evaporative salt build up in the soil. Though mangroves grow naturally in areas with inflow of both saline water and fresh water, high levels of salinity retard their growth.

In Figure 1.10, the spatial distribution of mangrove density, some topographic features and the frequency of tidal inundation of the different regions of the Henry's island according to their elevations are presented. In this figure, it can be seen that dense mangroves are located

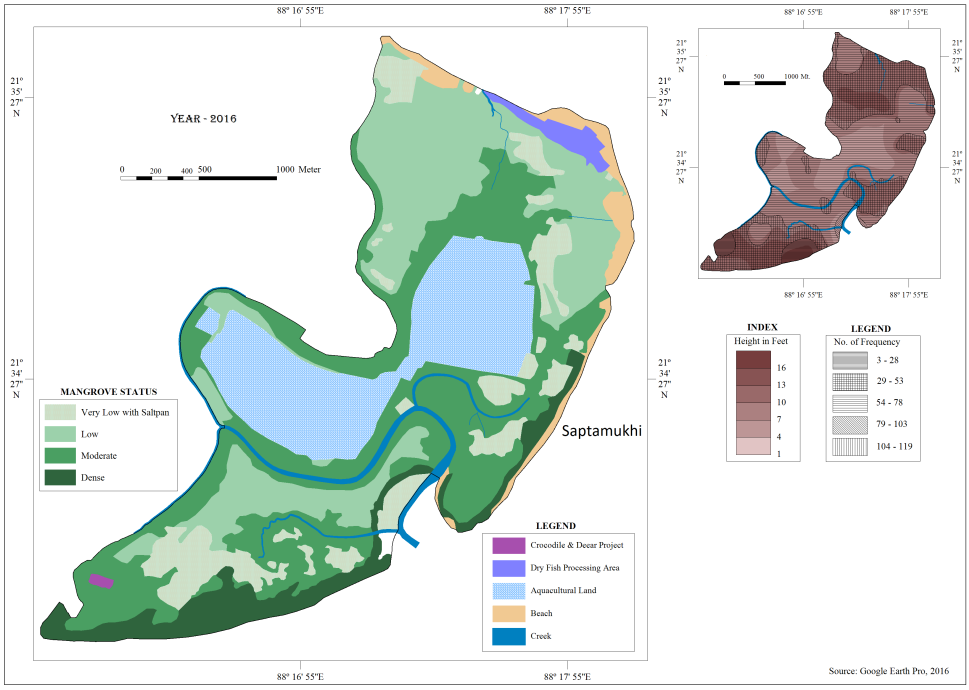

Figure 1.10: Distribution of mangrove vegetation and tidal inundation in the Henry's island.

along the shoreline, moderately dense mangroves are spread out all over the island except the northern part, and mangroves of low densities are found near the saline blank region and in the northern part. The presence of mangroves in the saline blank regions, which are located in the south-western, the eastern and the northern regions of the island, is very sparse. Also, it is reflected from Figure 1.10 that the regions with relatively higher elevations has the maximum concentration of vegetation concentration. Apart from the effect of coastal processes that make such relatively elevated regions favorable for mangrove growth, human influence has also played a beneficial role in the high density of mangroves in these particular regions of the Henry's island. Mangrove plantation is carried out by the forest department in these particular areas because in addition to having higher elevation, these regions are located directly next to the sea beaches, and having dense mangroves here would work for resisting shoreline erosion and also dampen the effect of storm devastation in the inland areas. From Figure 1.10, it is also seen that there is a close and negative association between mangrove density and the frequency of tidal inundation of a region. The causes of this negative association is explained above.

The mangrove zonation in the Patibania island depend on all the geomorphic, hydrological and climatic factors as in the case of the Henry's island, except human influence due to it being a reserve forest. The distribution of mangroves and the frequency of tidal inundation of the regions in the Patibania island are presented in Figure 1.11. From this figure, it can be seen

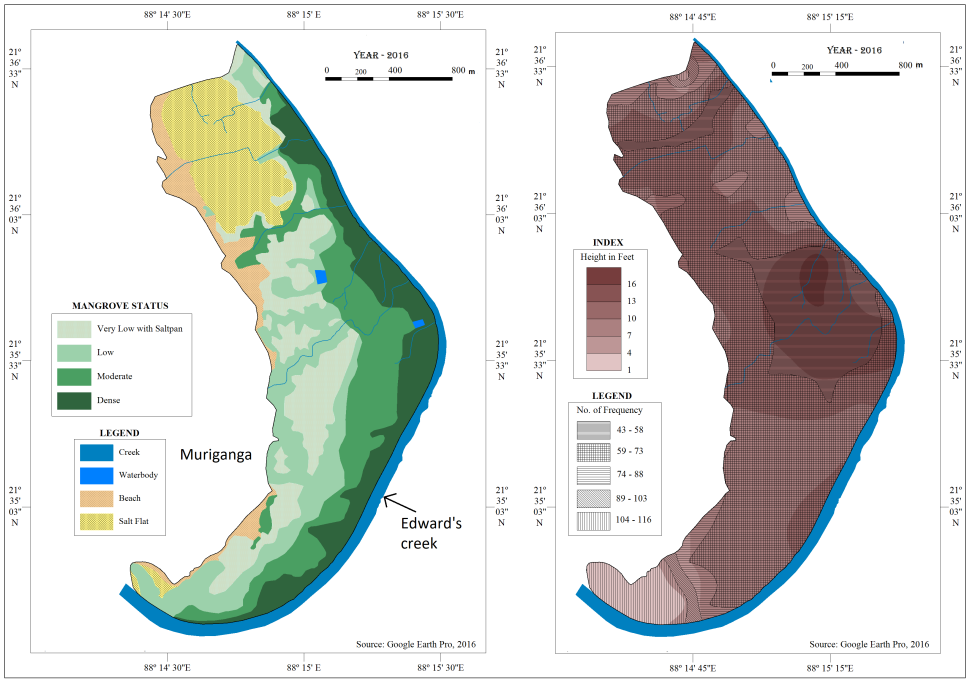

Figure 1.11: Distribution of mangrove vegetation and tidal inundation in the Patibania island.

that the zone with the highest elevation, which is located in the eastern part of the island, have the maximum concentration of mangroves. The frequency of tidal inundation increases from the east to the west as the elevation of the island gradually decreases in this direction. In the middle section of the island from the north to the south, the density of mangroves is low to very low. This region also has moderate to low elevation. It is notable that the mangrove growth is retarded in the northern middle section and the middle western part due to high levels of salinity. Low lying areas in the western and the central parts experience high frequency of tidal inundation, which increases the salinity level in the soil there. Consequently, only mangrove species that can tolerate high levels of salt grow there. The eastern part bounded by the bank margin ridge seldom experience tidal inundation, and therefore it is a dense mangrove zone with relatively low level of soil salinity.

In Figure 1.12, the schematic diagram of a transect of the Henry's island is presented, which depicts the various geomorphic features and vegetation growing in different elevation of this island. Similar schematic diagram of a transect of the Patibania island is presented in Figure 1.13. Both the transect charts are drawn from the west to the east to show the condition of mangroves and how they are varying with the change in the geomorphic settings. The vegetation characteristics and its growth are controlled by drainage, elevation and inundation. Along the transect in the Henry's island presented in Figure 1.12, in the western end there is a sand flat

covered in dense mangroves. Next to the sand flat, there are sand dunes with elevation up to 8 m. There is a mangrove swamp in this area. To the east of the sand dunes, there are ditches and ridges with elevation 3–4 m and covered in mangrove swamps. Next to the ditches and ridges, there is a creek, and on the banks of this creek, mangrove plantations are established. Beside the mangrove plantation, there is a sand flat with salt marsh vegetation. To the east of the sand flat, there is the Bakkhali creek, and on the eastern bank of the Bakkhali creek, there is a natural levee. The natural levee obstructs water from entering the saltpan on its east, and the saltpan has dwarf mangroves. To the east of the saltpan, there are sand dunes covered in dense mangroves and littoral vegetation. There is a creek, and on the eastern bank of that creek, a mud flat is present, which is covered by saltmarsh vegetation.

In Figure 1.13, at the western end there is the Muriganga estuary. To the east of the Muriganga estuary, there is a washover sand lobes with elevation 1 m and salt marsh vegetation. Next to the salt marsh vegetation, there is a zone with diversified vegetation. However, as one proceeds further east along this transect, there is a saltpan area formed in a depression, which has very less vegetation. The saltpan area has elevation 2 m and it is surrounded by regions with 3 m elevation. To the east of the saltpan area, there is a lagoonal flat, which has elevation 3 m, and is covered in moderately dense mangroves. Next to the lagoonal flat, there is a natural levee, which is covered in dense vegetation. This area has elevation around 5 m, and is the highest among the regions depicted in this transect.

To analyze the temporal change of the canopy cover in both islands, normalized difference vegetation index (NDVI) (Rouse et al., 1974) and moisture adjusted vegetation index (MAVI) (Zhu et al., 2014) are computed. The NDVI maps of the Patibania island are plotted in Figure 1.16 for the four years 2005, 2010, 2015 and 2019. The NDVI maps of the Henry's island are presented in Figure 1.17 for the same four years. The MAVI maps of the islands are prepared for the years 2000, 2010 and 2020, and presented in Figure 1.14 for the Patibania island and in Figure 1.15 for the Henry's island. NDVI is based on the spectral reflectance in two wavebands, red and near infrared, while the number of wavebands in the case of MAVI is three (red, near infrared and shortwave infrared) (Zhu et al., 2014). For this reason, and because the shortwave infrared band is sensitive to moisture levels, MAVI is often more effective in obtaining the leaf area index of a region (Zhu et al., 2014).

Based on the NDVI values over the four years, the areas covered by mangroves of different densities are calculated for both the islands, and these are presented in Table 1.1 for the Patibania

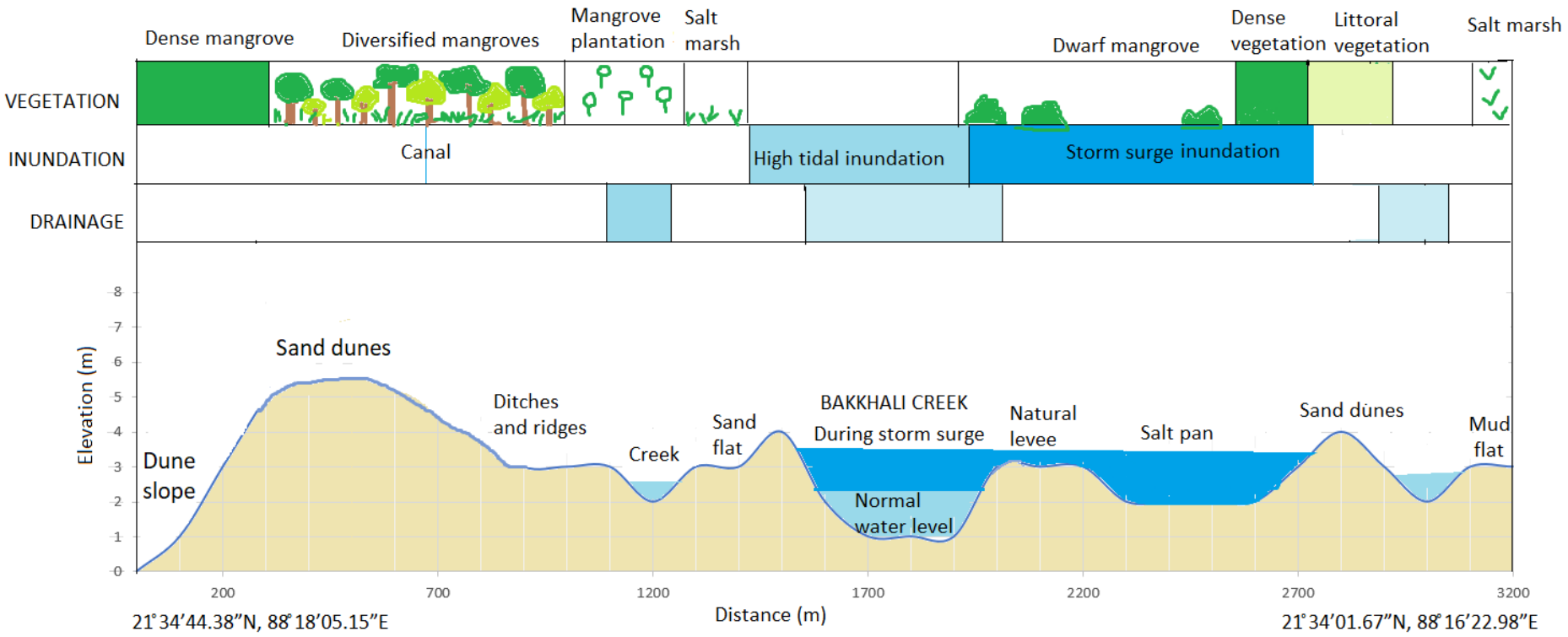

Figure 1.12: Schematic diagram of a transect in the Henry's island.

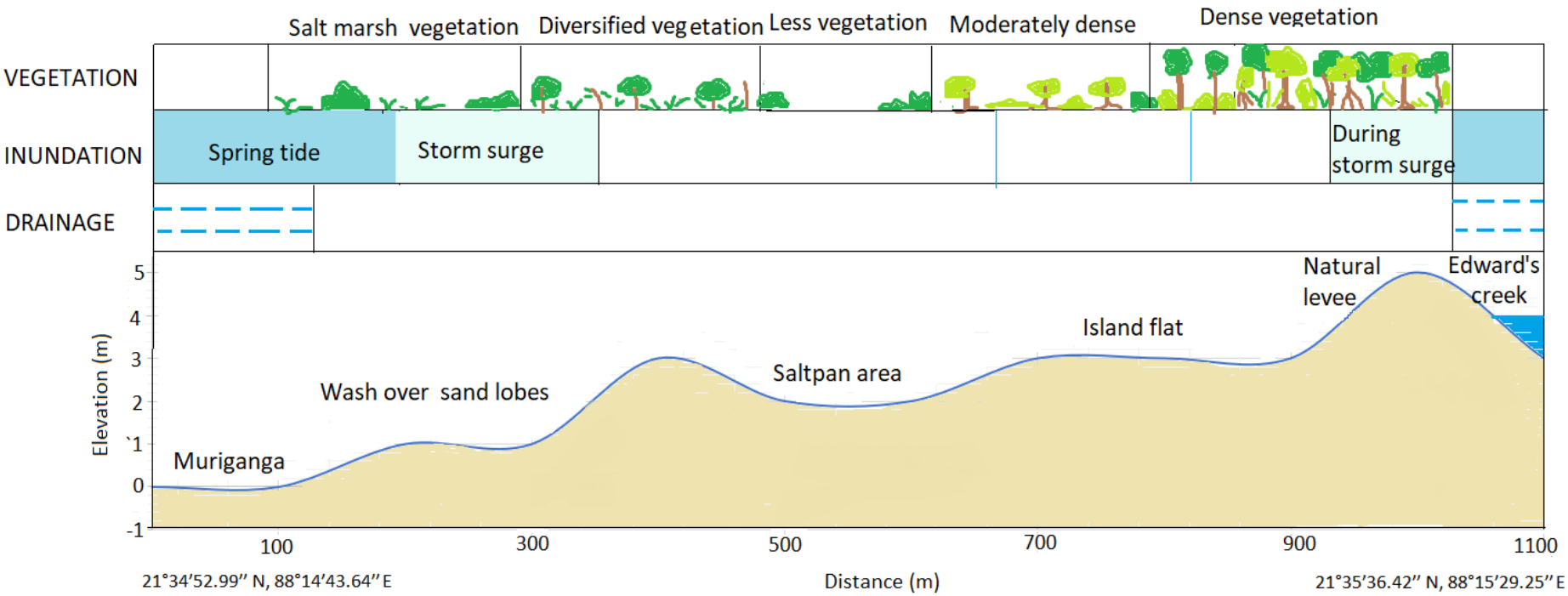

Figure 1.13: Schematic diagram of a transect in the Patibania island.

island and in Table 1.2 for the Henry's island. In Table 1.1, one can see that the area covered by dense mangroves in the Patibania island was highest at 2005. It decreased sharply in 2010 and then partially recovered by 2015. In 2019, it decreased marginally. The areas covered by mangroves of moderate and low densities both exhibit decreasing trends from 2005 to 2015, and then both increase in 2019. The are covered by mangroves of very low density sharply rose in 2010, then marginally decreased in 2015 and substantially decreased in 2019. Major part of these changes can be explained by the devastation brought by the cyclone Aila in 2009, which destroyed much of the mangroves. Due to this, the areas covered by dense mangroves, moderate mangroves and even mangroves of low density all decreased substantially in 2010, while the area under mangroves of very low density increased significantly. After that, recovery took place and the area under dense mangroves increased by 2015, while the areas under mangroves of moderate, low and very low densities decreased. By 2019, the area under dense mangroves decreased marginally and the area under mangroves of very low density decreased considerably, but the areas under mangroves of moderate and low densities increased. Overall, these changes depict the recovery of the mangrove ecology after its decimation by Aila but also the secular degradation of mangroves over time in the Patibania island, presented in the fact that the area under dense mangroves decreased from 2015 to 2019, and that both areas under dense mangroves and mangroves of moderate densities were smaller in 2019 compared to 2005, while the areas under mangroves of low and very low densities were higher in 2019 compared to 2005.

Table 1.1: Area of mangrove zones (in km^2) in the Patibania island based on NDVI.

Area of mangrove zones (in km^2)				
Mangrove Status	2005	2010	2015	2019
Dense	0.835	0.776	0.815	0.812
Moderate	1.194	0.985	0.981	1.002
Low	0.982	0.956	0.939	1.102
Very Low	1.021	1.32	1.31	1.139

In Table 1.2, one can find very different changes in the status of mangrove density over the four years compared to the Patibania island. Here, the areas under dense mangrove sharply rose from 2005 to 2010, while the areas under mangroves of moderate and low densities also

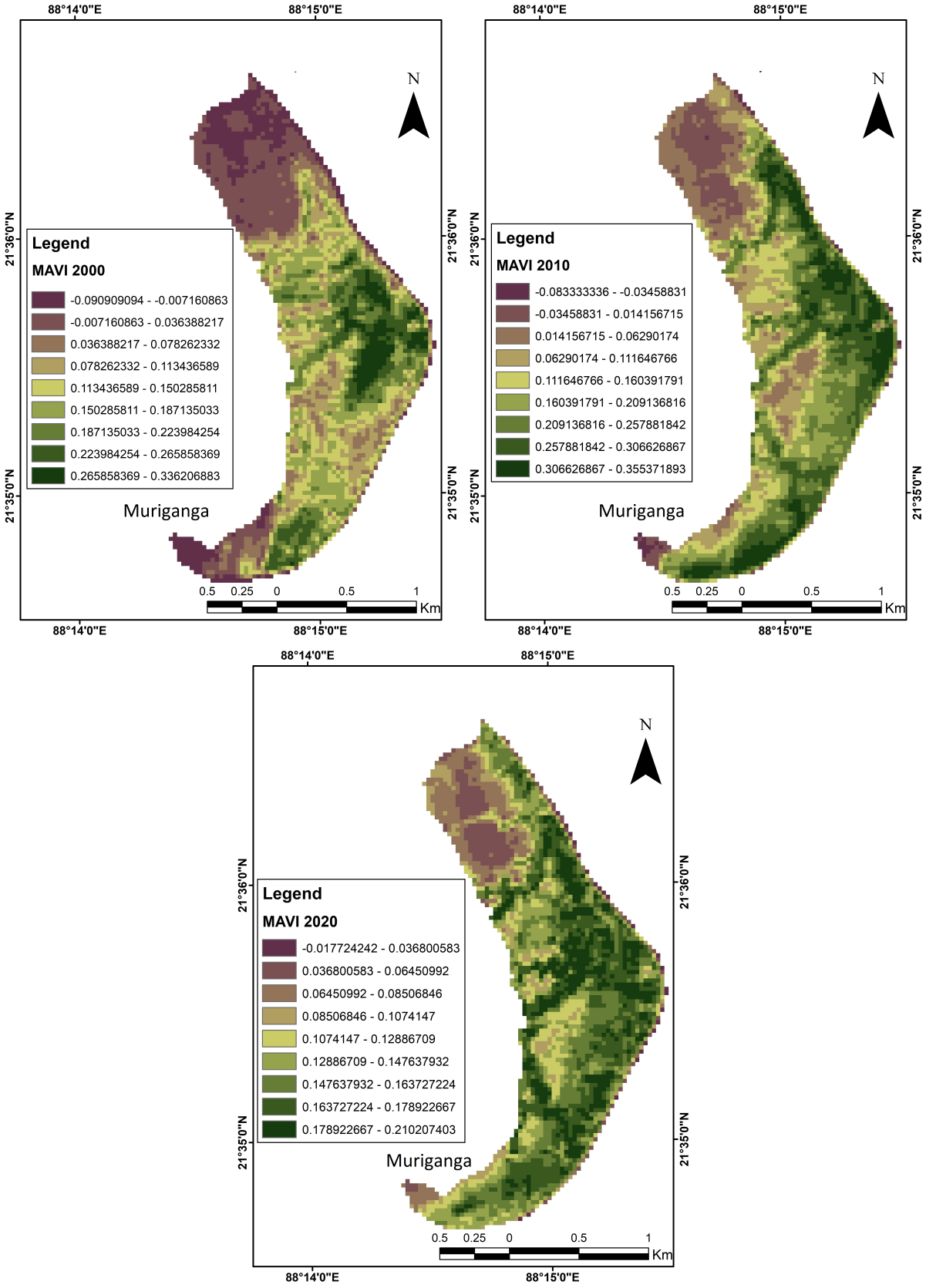

Figure 1.14: MAVI maps of the Patibania island for the years 2000 (left), 2010 (middle) and 2020 (right).

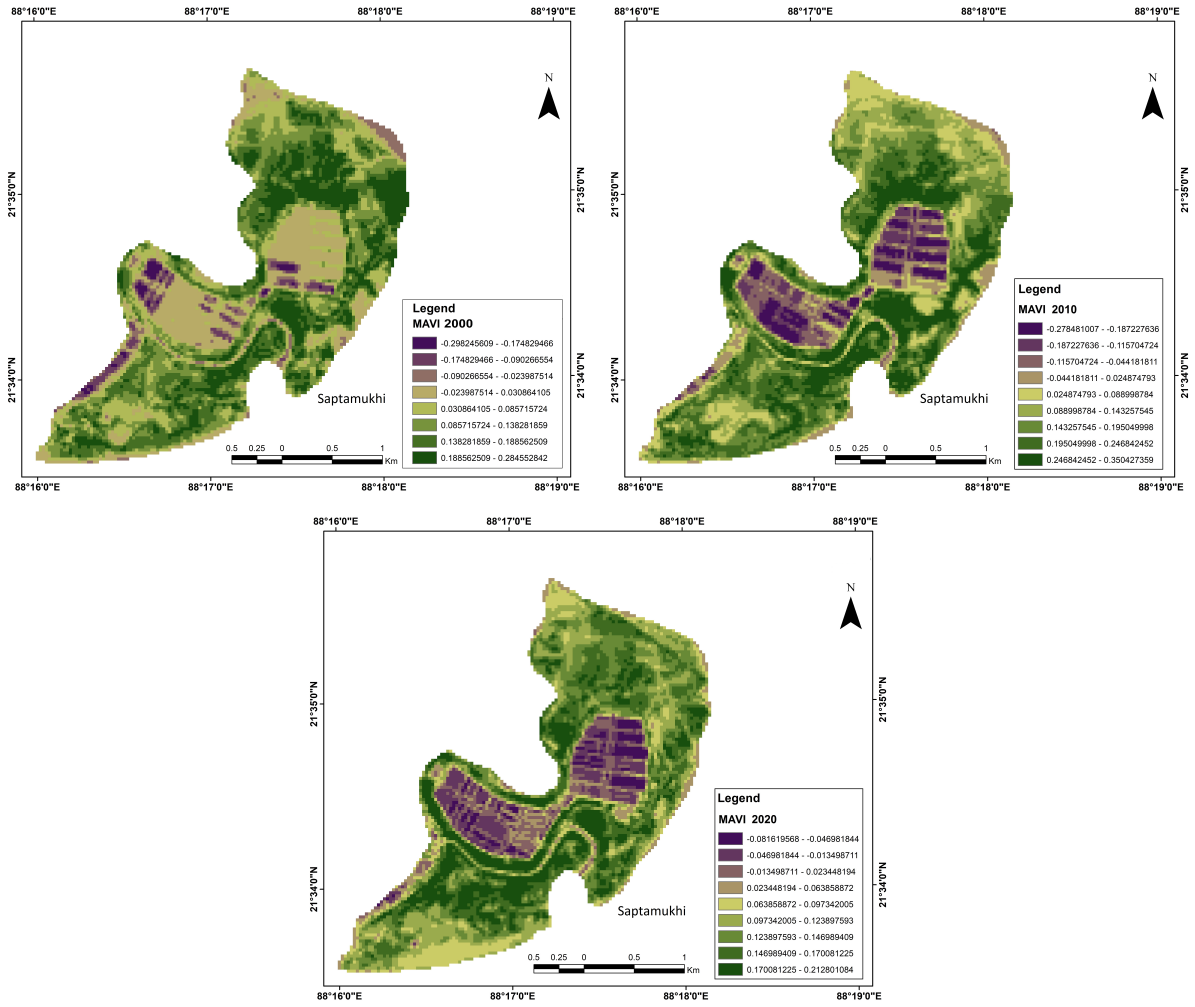

Figure 1.15: MAVI maps of the Henry's island for the years 2000 (left), 2010 (middle) and 2020 (right).

Table 1.2: Area of mangrove zones (in km^2) in the Henry's island based on NDVI.

Area of mangrove zones (in km^2)				
Mangrove Status	2005	2010	2015	2019
Dense	1.166	1.718	1.964	1.749
Moderate	0.921	0.967	1.168	1.22
Low	1.349	1.737	2.011	1.654
Very Low	2.168	1.907	1.281	1.804

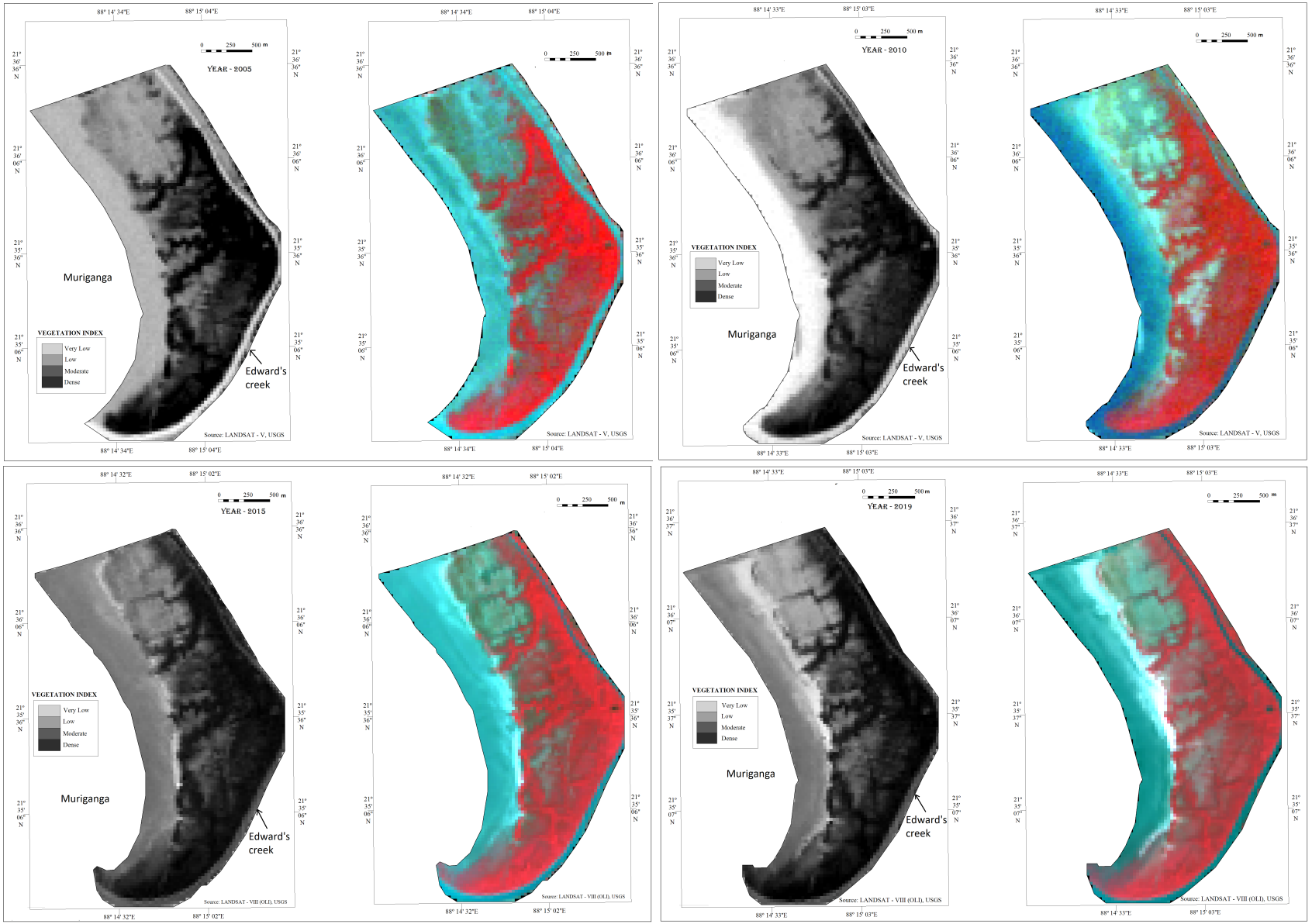

Figure 1.16: NDVI maps of the Patibania island for the years 2005 (top left), 2010 (top right), 2015 (bottom left) and 2019 (bottom right).

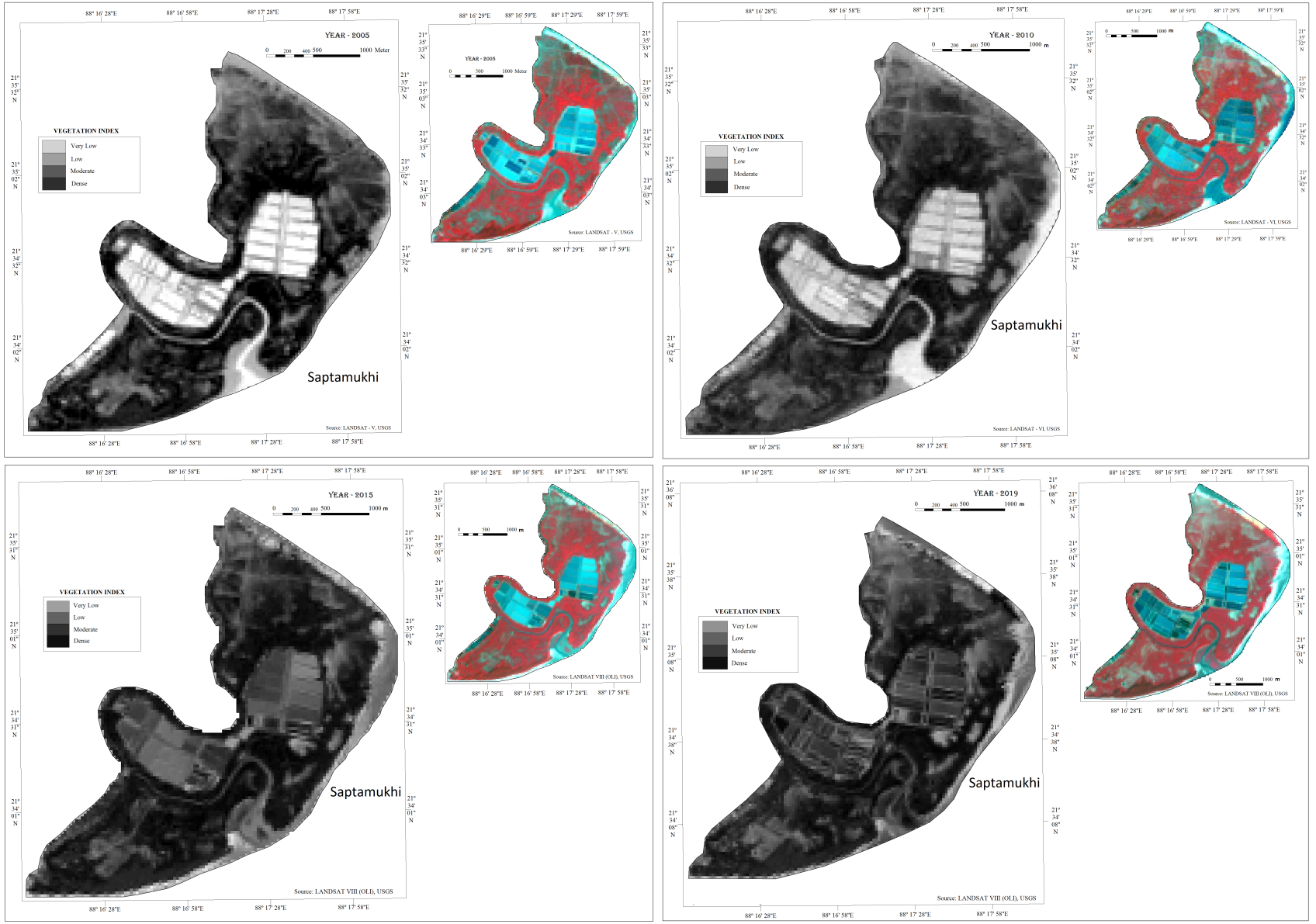

Figure 1.17: NDVI maps of the Henry's island for the years 2005 (top left), 2010 (top right), 2015 (bottom left) and 2019 (bottom right).

increased. Only the area under mangroves of very low density decreased from 2005 to 2010. This trend continued till 2015. However, from 2015 to 2019, the areas under dense mangroves and mangroves of low density decreased, while the areas under mangroves of moderate and very low densities increased. This strikingly different change in mangrove distribution can be explained by the intensive afforestation activities carried out by the government and the local community after the devastation of Aila in 2009. One can see that this afforestation completely nullified the destruction caused by Aila, and the density of mangroves is higher n 2010 than 2005. The status of mangrove degraded somewhat from 2015 to 2019. However, mangrove concentration in 2019 is higher compared to 2005.

These observations clearly reflect the extent of human impact on the mangroves. Because the devastation from Aila was extensive and the Henry's island has significant human presence, significant afforestation activities were carried out in the Henry's island. But the Patibania island is almost completely off-limits to humans due to it being a reserve forest, and hence there was no economic or societal interest in executing a similar planned afforestation drive there. In the Patibania island, the recovery of mangrove occurred in the natural way. It turned out that the artificial afforestation by humans in the Henry's island was considerably more extensive than the natural one in the Patibania island. The conclusion that one can draw from these observations is that while mangroves face adverse pressures from ongoing climatic, hydrological and related geomorphological processes and anthropogenic activities, concerted human effort can nullify the negative influences.

While Table 1.1 and Table 1.2 depict the overall changes in mangrove density, the NDVI and the MAVI maps also depict the spatial distribution of mangroves and its change over time. In the NDVI maps of the Patibania island in Figure 1.16, it can be observed that vegetation has slowly proliferated in the northern part of the Patibania island, which was almost barren in 2000. The same process is more clearly reflected in the MAVI maps in Figure 1.14. It is also reflected in the MAVI maps that in 2000, in most of the Patibania island, the vegetation concentration was low, while places were densely covered by mangroves. However, vegetation concentration started increasing in almost all the regions of the island, while the middle eastern part, which was densely covered by mangroves in 2000, has undergone some decrease in the density of mangroves by 2020. In the NDVI maps of the Henry's island in 2010, it can be observed that the vegetation density decreased in the eastern shoreline adjacent to the Saptamukhi river estuary, which would have faced the brunt of the destructive forces of Aila in the previous

year. The same is true for the banks of the mouth of the creek, which flows through the island. However, both of these two areas show signs of a gradual recovery of vegetation in the NDVI maps of 2015 and 2019. In the MAVI maps of the Henry's island, a decrease in the extent of vegetation in the southern seashore can be observed in 2020 compared to 2000 and 2010. Also, the density of mangroves in the northern areas of the Henry's island has undergone a gradual decline from 2000 to 2020. Overall, the spatial variation of mangrove density has decreased from 2000 to 2020 in the Henry's island.

1.6 Future threats to the low lying islands

Erratic weather events, climate change and the associated change in the mean sea level affect the livelihood of the communities and the biodiversity of the low lying coastal zone in Sundarbans. The rise of the sea level is a major impact of climate change, and is one of the the most important concern around the world. The lives of people are at stake with the destruction of resources as well as biodiversity. A 30 cm rise in sea level would increase flood intensity by 36-58% all along the coastal lines (Rawat et al., 2016). IPCC projections assumed that sea level rise show scenarios from 0.3-1.1 m by the year 2100 with a best estimate of 0.66 m rise, which can inundate low-lying wetland, erode sea shores, increase salinity, rise coastal salt water tables, and exacerbate coastal flooding and also storm damage. Barnett and Campbell (2010) have articulated the challenges before island communities to "adapt, to sustain their needs, rights, and values" and the challenges before international community to reduce greenhouse gas emissions and support island communities to adapt. Globally, average sea level rose between 0.1 and 0.2 m during the 20th century and based on tide gauge data, the rate of global mean sea level rise was in the range of 1.0-2.0 mm/year compared to an average rate of about 0.1-0.2 mm/year over the last 3,000 years (Nicholls and Leatherman, 1996). Warrick and Oerlemans (1990) estimated a global sea level rise in the order of 0.5-3 mm per year. Considering the present relative sea level rise at 3.14 mm per year, it is estimated that by the year 2050, the compound sea level elevation will become close to the 1 m scenario of Broadus (1993).

Most of the south-western Sundarban region lies within 5 m of elevation (Paul, 2002). However, often the normal tidal amplitude itself exceeds 5 m over the whole of the coast of West Bengal, and in Sundarban region, it may even exceed 6 m (Paul, 2002). Thus, from normal tide action alone, vast regions of Sundarban would be prone to frequent inundation, discarding

the gradual effects of sea level rise due to climate change and subsidence of the delta from the auto-compaction of sediments. Most of the lowlands in Sundarban is protected from tidal inundation by extensive earthen embankments rising up to 3 m above the area behind them (Paul, 2002). However, other human activities like upstream dam building and groundwater extraction worsen the already existing risks of inundation of the lowlands. Upstream dams considerably reduce the flow of sediments, and over-exploitation of groundwater aids in the subsidence of the delta.

To assess the impact of sea level change in the coastal areas of Sundarban, several aspects of Sundarban was analyzed in (Hazra et al., 2002) including temperature regime, occurrence of high intensity climatic events like cyclones and shoreline change. According to their estimation, erosion zones are most prominent among the sea facing southern islands of Sundarban. Erosion and submergence dominates the southern parts of the islands in Sundarban. Paucity of sediment supply,relative sea level change main cause for the erosion and submergence of island. Since cyclonic storm surges will become more severe with the rise of sea level and most of them occur during the pre and post-monsoon periods, the most serious problems will be faced during this time (Hazra et al., 2002). The effect of storm surge would be severe for the areas which are located along the coastline in the monsoonal period. South-East part of Namkhana, Mousuni island, Jambudip strongly exposed to the coastal erosion due to sea level change presently (Hazra et al., 2002). Land use change like reduction of land area within the coastal regulatory zones, degradation of mangrove and increasing salinization, erosion and submergence of beaches and mud flats are among the principal outcomes sea level rise presently. Apart from these islands, ecology will be suffered mostly due to sea level rise and changing climate. Keeping the view of the present changes in the coastal tract of Sundarban like temperature, sea level, coastal configuration, salinity, forest cover, land use, population, agricultural and fish productivity, the changes in shore line of the island system vis a vis sea level appears to be of prime importance in assessing the vulnerability of the fragile eco system in a climate change scenario. High frequency of cyclonic storms increase surge height inundate coastal belt. Increase surface temperature over Bay of Bengal at 0.019°C/year, which increases the rise of the relative sea level at 3.14 mm/year around the Sagar island, thus accelerates coastal erosion and submergence of island.

Due to coastal erosion and flooding, around 30,000 people are feared to be rendered homeless from Sagar Island alone, turning into environmental refugees. Considering the whole of

Sundarban with the existing trend of population rise and reclamation, this number may touch 0.1 million mark by 2050. Mangrove forest cover is predicted to diminish further along with degradation of the existing species combination. Agriculture and fish production may also face a serious threat.

1.7 Literature review

Sundarban has long drawn researchers due to its vast and rich mangrove forests, fertile alluvium soil but also salinization, dynamic and adaptable yet fragile mangroves, conspicuous geomorphic features, wide rivers prone to channel avulsion, and some of the densest human habitation in the world coexisting with several endangered species. The characteristics of mangroves like their salt tolerance, biological productivity and ecosystem services have pulled many researchers to investigate them. Here, the relevant and notable research articles related to the current area of research are described by grouping them in the following categories.

Physical background of Sundarban: One of the earliest works describing the physical features and local fauna is by Rainey (1891). In Das (2015), the physical settings of Sundarban is described, and the ecology is studied in Rahman and Asaduzzaman (2010) and Aziz and Paul (2015). The geology of the Sundarban region and its evolution are intricately connected to those of the larger Ganga-Brahmaputra basin, especially its lower part, which is often called the Bengal Basin. The changing sedimentary geology and other physical features of the Bengal Basin and related tectonics, which have a deep impact on the Sundarban region, are studied in Alam et al. (2003). Allison et al. (2003) and Patrick (2016) investigated the evolution and the landforms of the Ganga-Brahmaputra lower delta plain, most of which is comprised of Sundarban. In Ghosh et al. (2015), the history and conservation strategies of the mangrove forests in Sundarban is described. In Ganguly et al. (2006), the geomorphology of the Sundarban estuarine region and its change over time are studied using remote sensing data. The physical, chemical and biological aspects of the estuarine ecosystem in Sundarban and their interactions are studied in Manna et al. (2012). In Quader et al. (2017), the spatio-temporal evolution of the mangrove density in Sundarban is investigated. Bandyopadhyay (2019) studied aspects of the geomorphology and the mangrove ecology in Sundarban.

Coastal morphodynamics and geomorphic settings of Sundarban: Being located in a coastal estuarine region, the interplay of the morphology and the hydrodynamics processes moulds the

geomorphic settings of Sundarban. Coastal morphodynamics was investigated in Guisado-Pintado et al. (2020). In Agardy and Dayton (2005), the various geomorphic settings of a coastal system were described. Boon III and Byrne (1981) studied the morphodynamics of coastal inlet systems. The evolution of the coastal morphodynamics is investigated by Carter and Woodroffe (1994) and Cowell and Thom (1994). Masselink and Short (1993) investigated and developed a model to study beach morphology. Dodd et al. (2003) employed stability models to investigate the coastal morphodynamics. Jackson et al. (2005) investigated geological control of beach morphodynamics, while Lercari and Defeo (2006) studied the diverse ecology in the beach. Banerjee (1998) and Paul (2002) studied the coastal region of Sundarban, including its geomorphology, environment and anthropological aspects. In Ghatak and Sen (2010), a morphological model of an island in the Hooghly estuary is developed and its effectiveness is examined. In Mondal et al. (2015), the morphodynamics of the coastal stretch of the south-western Sundarban region is studied.

Tidal flat settings: Tidal flats are one of the most prominent geomorphic features of an estuarine environment. In Shinn (1983) and Reise (2012), several features of tidal flats and the supported ecology are described. In Thompson (1968) and Yang et al. (2005), sedimentation on tidal flats is studied. In Nakada et al. (2011), water circulation below tidal flats is investigated. Hu et al. (2015) employed a dynamic equilibrium theory for short and long-term forecast of tidal flat morphodynamics. Anthony and Héquette (2007) studied the grain-size characterization of sand from several coastal settings including tidal flats. In Bádenas et al. (2018), a facies model of an open-coast tidal flat is developed. In Peterson and Vanderburgh (2018), the impact of the tectonic processes on the depositional patterns of a tidal flat is investigated. In Oms et al. (2016), the transitional environments of a tidal flat is studied.

Climate variability and impact on mangroves: Mangroves are highly adaptable to changing environment conditions, however, the ongoing climate change puts them under very unfavorable conditions and reduce their proliferation over time. In Field (1995), the potential impact of climate change on mangroves is studied. In Choudhury et al. (2019), the sensitivity of the Sundarban mangrove ecosystem to the changes in the local climate is investigated. The effect of climate change on the flow of Ganga, one of the principal rivers of the Sundarban region, is studied in Goodbred Jr (2003). Lloret et al. (2008) studied the effect of climate change on eutrophication, which creates unfavorable environments for mangroves. Sadik and Rahman (2009), Mahadevia Ghimire and Vikas (2012), Bhattacharjee et al. (2013), DasGupta and

Shaw (2013), Guha et al. (2015), Alam et al. (2016) and Neogi et al. (2016) investigated the impact of climate change on the mangrove ecology, aquatic life and human population in Sundarban. In Ghosh (2018), the spatio-temporal changes in the geomorphology of the south-western Sundarban in the context of the ongoing climate change is studied. The impact of climate change on other mangrove ecosystems was investigated by Alongi (2015) and Ward et al. (2016). In Chakraborty et al. (2014), the effects of global warming on the mangroves in Sundarban are studied using different physical and chemical markers and assessment tools. Some of the most important drivers of the ongoing climate change are the greenhouse gasses, including carbon dioxide and methane. In Mukhopadhyay et al. (2002), the impact of the mangroves in Sundarban on the carbon dioxide and methane contents in the local atmosphere is investigated. In Erwin (2009), the role of wetland restoration in coping with the ongoing climate change is studied. In Danda et al. (2011), an initiative was taken to develop a workable action plan to cope with the pressures of the ongoing climate change on the Sundarban biosphere.

Saltmarsh vegetation and its biogeography: Saltmarshes are often situated at the boundary of the mangroves, and they are potential sites for mangrove colonization. In this way, saltmarshes and mangroves share an intricate relationship. Silvestri and Marani (2004) described the morphology of the saltmarshes and discussed remote sensing techniques to retrieve information about the saltmarshes. Moffett et al. (2010) investigated how the saltmarsh vegetation zonation is affected by soil characteristics and topography. Lugendo (2016) investigated the inter-relationship between mangroves and saltmarshes. Saintilan and Williams (1999) investigated the process of mangrove colonization in saltmarshes. Simas et al. (2001), Hartig et al. (2002), Kirwan and Mudd (2012) and McKee et al. (2012) investigated the effects of climate change and anthropogenic activities on the saltmarshes around the world. In Viswanathan et al. (2020), the distribution and zonation pattern along with species composition of the saltmarsh vegetation in India are studied. Aysha et al. (2015) studied sediment and carbon accumulation in the saltmarshes in Sundarban. Kim et al. (2011) investigated the potential of the saltmarshes serving as an indicator of climate change. In Davis and Lovell (2012), aspects of microbial life in a saltmarsh environment is investigated. In McKee and Vervaeke (2018), the impact of the dynamics between saltmarshes and mangrove ecosystems on the vulnerability of a subtropical wetland to sea level rise is investigated.

Evolution of saltpans and their characteristics: Emergence of saltpans in mangrove areas hinders the growth of mangroves. Within and around the saltpans in a relatively small area,

significant variation is observed in the vegetation characteristics. In Escapa et al. (2015), the process of saltpan formation in saltmarshes and its bio-geomorphic aspects are investigated. The evolution of a saltpan was studied in Metcalfe (1993) by examining the diatoms present in a core sample obtained from the saltpan. Marchionni et al. (2009) developed methodology to analyze the characteristics of the saltpans using remote sensing tools. Saltpan evaporites were investigated in Lowenstein and Hardie (1985). Dias et al. (2014) discussed the possibilities of employing artificial saltpans as habitats of shorebirds. Singaraja et al. (2014) described the role of saltpans in groundwater contamination.

Mangrove response to sea level change: Sea level rise pose a significant threat to the survival of the mangrove ecosystem. Hazra et al. (2002) described the changes in the sea level in Sundarban. Raha et al. (2014) provided a time series study of the rise in sea levels and island submergence in Sundarban. In Gilman et al. (2007), an assessment of the response of mangroves in the face of the projected rise in sea levels is done along with historical reconstruction of past shorelines. Woodroffe (2018) assessed the response of mangroves to sea level rise from palaeoecological reconstructions. Saintilan et al. (2020) estimated the threshold of mangrove survival under rapid rise in sea level. Woodroffe et al. (2016) studied sedimentation in mangrove areas and the response of mangroves to sea level rise.

Impact of salinity on mangroves: Although mangroves grow where there is supply of both saline water and freshwater (Mitra, 2018), too high salinity works against the growth and the proliferation of mangroves. Mitra et al. (2010) and Dasgupta et al. (2017) investigated the impact of salinity on mangroves in Sundarban. Chand et al. (2012) studied the effect of saline water inundation on local agriculture. Yang et al. (2013) studied the salinity gradient and its influences on inundation tolerance thresholds of mangroves. In Banerjee et al. (2017), the impact of the salinity variation induced by climate change on a mangrove species is studied. In Barik et al. (2018), Peters et al. (2020) and Rahman (2020), the relationship between salinity and water availability and mangrove distribution is studied. Aspects of soil salinity estimation are investigated in Liu et al. (2018).

Restoration of mangroves: Mangroves are considerably degraded due to anthropogenic and climatic influences, and their management and restoration are of paramount importance. Ellison (2000) assessed the effectiveness of the contemporary mangrove restoration projects. McKee and Faulkner (2000) investigated the restoration of the biogeochemical functions of the mangrove forests. Iftekhar and Islam (2004) developed a strategy for the management

of mangroves in Bangladesh. Lewis III (2005) studied ecological engineering techniques to restore mangroves. Bosire et al. (2008) provided an overview about the functionality of restored mangroves. Datta et al. (2012) proposed community based mangrove management and argued about its usefulness. Hossain et al. (2017) discussed a bio-economic modeling technique for the restoration of mangroves. Bosire et al. (2003) investigated the natural colonization of plant species in restored mangrove ecosystems. In Gopal and Chauhan (2006), the biodiversity in the Sundarban mangrove ecosystem and ways of its conservation are studied. In Sahu et al. (2015), the implications of the loss of mangrove habitats in India are investigated. In Islam and Wahab (2005), the status of the mangrove ecosystem in Sundarban is reviewed and the need for proper conservation strategies is stressed. In Iftekhar (2008), strategies for the management of mangrove ecosystems in South Asian countries are described. In Ekka and Pandit (2012), the economic and financial aspects for the restoration of mangroves in Sundarban are studied. In Ranjan (2019), the importance of community engagement in mangrove restoration in Sundarban is highlighted. The properties of soil and vegetation of mangrove ecosystems in Sundarban under different management systems are investigated in Datta and Deb (2017). The utility of native salinity tolerant grass in the restoration of mangrove habitats in Sundarban is studied in Begam et al. (2017). In Alam et al. (2014), the suitability of certain mangrove species to be used in plantation projects for the restoration of mangroves is examined.

Biomass estimation of mangroves: Occurring in humid tropical or subtropical climates, a mangrove ecology is biologically very productive. It can remove a large amount of carbon from the atmosphere. Komiyama et al. (2000) investigated the ratio of biomass of the top and the root of a mangrove ecology. Goodale et al. (2002) described the forest carbon sinks in the northern hemisphere, which include the mangroves. In Donato et al. (2011), it was observed that mangroves are some of the most carbon-rich tropical ecosystems, capturing and storing carbon in a disproportionately large amount compared to the relatively modest area occupied by them. Machiwa and Hallberg (2002) developed an empirical model for the captured organic carbon in a mangrove forest affected by human activity. Komiyama et al. (2005) described methods for estimating the weight of a tree in a mangrove habitat. Komiyama et al. (2008) provided a review of the productivity and biomass of a mangrove along with methods to estimate the biomass. Rahman et al. (2015) and Kamruzzaman et al. (2017) described about the total biomass available in Sundarban. In Chanda et al. (2016), the projected blue carbon stock captured in the Bangladeshi part of Sundarban mangrove ecosystem after a century is investigated. In Khan

et al. (2007), methods of estimating the carbon and nitrogen content in a mangrove species were described. In Banerjee et al. (2013), allometric equations for biomass estimation based on salinity is developed for the mangroves in Sundarban.

Mangrove ecosystem services: Mangroves are of vital economic importance to the people cohabiting in the mangrove region. They provide a large amount of ecosystem services. Lee et al. (2014) described the ecological role and the ecosystem services provided by mangroves. Jayanthi et al. (2010) described the role of mangroves in aquacultural developments in the mangrove area. Alongi (2011) described how the process of carbon-payment can be employed for the mangrove conservation. Mukherjee et al. (2014) discussed about the valuation of the ecosystem services provided by mangroves. Lee et al. (2014) described the ecological role and services of a mangrove ecosystem. Alongi (2014) discussed about carbon cycling and storing it in the mangroves. In Hossain et al. (2016), the ecosystem services of the mangrove forests in Sundarban are detailed. The high rate of sedimentation results in discontinuities in the estuarine streams, which reduce water flow and consequent degradation of ecosystem services. Restoring water flow in those streams would result in an improvement of ecosystem services, and Bhadra et al. (2017) described a way to employ geo-informatics to identify the blocked estuarine streams. The anthropogenic damage to the mangrove ecology in Sundarban is studied in Jalais (2004). Other notable works on the ecosystem services of mangroves are by Mandal and Nandi (1989) studied the fauna of Sundarban. Kathiresan and Bingham (2001) studied the biological aspects of the mangrove ecosystem in Sundarban. Vittal and Sarma (2006) investigated the fungal ecology and its biological diversity in the mangroves of Sundarban. In Mazda et al. (2007), the physical processes in mangrove habitats and their effects on the preservation of mangrove ecosystem services are studied. Manna et al. (2010) and Prasad (2012) investigated the dynamics of the eutrophication and its potential harmful effects on the mangrove ecosystem in Sundarban. Chauhan and Gopal (2014), Brahma and Mukherjee (2016), , , Willemsen et al. (2016), . Mandal et al. (2012) and Mandal et al. (2013) studied the nitrogen dynamics in mangrove habitats of Sundarban.

Hydrological model: Mangroves grow in the regions where both saline water and freshwater are available. The optimal growing condition of a mangrove species requires a certain balance in saline water intrusion and freshwater influx. So, constructing a hydrological model for the study area is required to examine the water availability and the balance of freshwater and saline water there. In Döll et al. (2003), a global global hydrological model was developed.

Wahid et al. (2007) described the hydrological monitoring in the Bangladesh part. Todini (2007) discussed about hydrological catchment modeling. Pechlivanidis et al. (2016) developed a multi-basin hydrological modeling, Lüke and Hack (2017) discussed about ways to model hydrological ecosystem services. In Donohue et al. (2007), the importance of the role of vegetation dynamics in a hydrological model is demonstrated. In Mandal et al. (2012), mangrove litter nitrogen cycling was investigated through hydrological models.

1.8 Research gap and research questions

In Ganguly et al. (2006), 10 geomorphic features of south-western Sundarban were identified. But detailed study of the other geomorphic settings was not covered in their work. Hazra et al. (2002) mentioned the impact of sea level changes over Sundarban and its associated land forms. He identified several formations of saltpans within mangrove swamp, but a detailed study of saltpan formation was not undertaken. The present research work shall identify the formation process and stages of development of the saline blanks in the Henry's island and the Patibania island. Continuous monitoring and field work reveal that characters of the saline blanks in both islands are different, In spite of having the same temperature, rainfall and humidity, physico-chemical properties of soils in the two islands are significantly different.

In the high evaporative conditions, salt crystals are found on the leaf of Avicennia marina in the Henry's island in the month of May. But no such salt crystals are found in the saline blanks of Patibania island in the same month. This yields the question that why salt crystals are not found in all saline blanks of these two islands. Another question related to the salinity levels is that why the saltpans of the Henry's island do not have any mangroves in the central part of the saline blank. Mangrove plays unique role in the distribution pattern within saltpan area.

Rahman et al. (2011a) identified several signature of mangrove adaptation with changing sea level change in Sundarban but they did not mention the succession of mangrove within different geomorphic settings of the islands. This research work would identify the reason behind the different succession level of mangroves within various physiographic settings and different sub systems in the both islands. Though several geographers have studied the physical background of Sundarban and its coastal process but no one emphasized on the issues of the tidal drainage loss. This factor is one of the important causes for the degradation of mangrove and growth of saltpan. Therefore impact and amount of tidal drainage loss in the Henry's and the Patibania

island is a major issue for this research work. Lewis III (2005) probably the first one mentioned the process ecological engineering technique to restore mangrove but why this process should be incorporated in Sundarban was not discussed by any other geographer in Sundarban. Several management techniques to conserve mangroves have been discussed in different literature but which techniques are most useful in the Henry's and Patibania have not been discussed in details. Major contribution of this paper would be the identification of main factors for the degradation of mangroves in both Henry's and Patibania islands and also to mention several suitable techniques to restore the regeneration process of mangroves spatially.

1.9 Objectives of the present study

The chief objectives of the present study are:

- To examine the modern coastal process and temporal change of the islands.
- To identify the geomorphological settings of the islands.
- To identify the coastal environments and regional settings of the islands.
- To investigate the issues of environmental assessment and physiographic settings
- To assess the island hydrology and regional changes of the islands.
- To ascertain the future direction of coastal resource management and sustainable development.

This research will highlight the impact of regional settings on the island, especially mangrove distribution and its zonation. Furthermore, the study involves spatial and statistical techniques for the analysis of the collected data. This has not been done before in this region. This would facilitate the system and analytical understanding of mangrove conservation through proper knowledge and information.

1.10 Materials and methods

This section describes the materials and method used for the research work. The methodology adopted in this work is divided into pre-field, field and post-field study. In pre-field work, literature review on several aspects was done. Hooghly tidal data for 2018 and 2019 of station Sagar

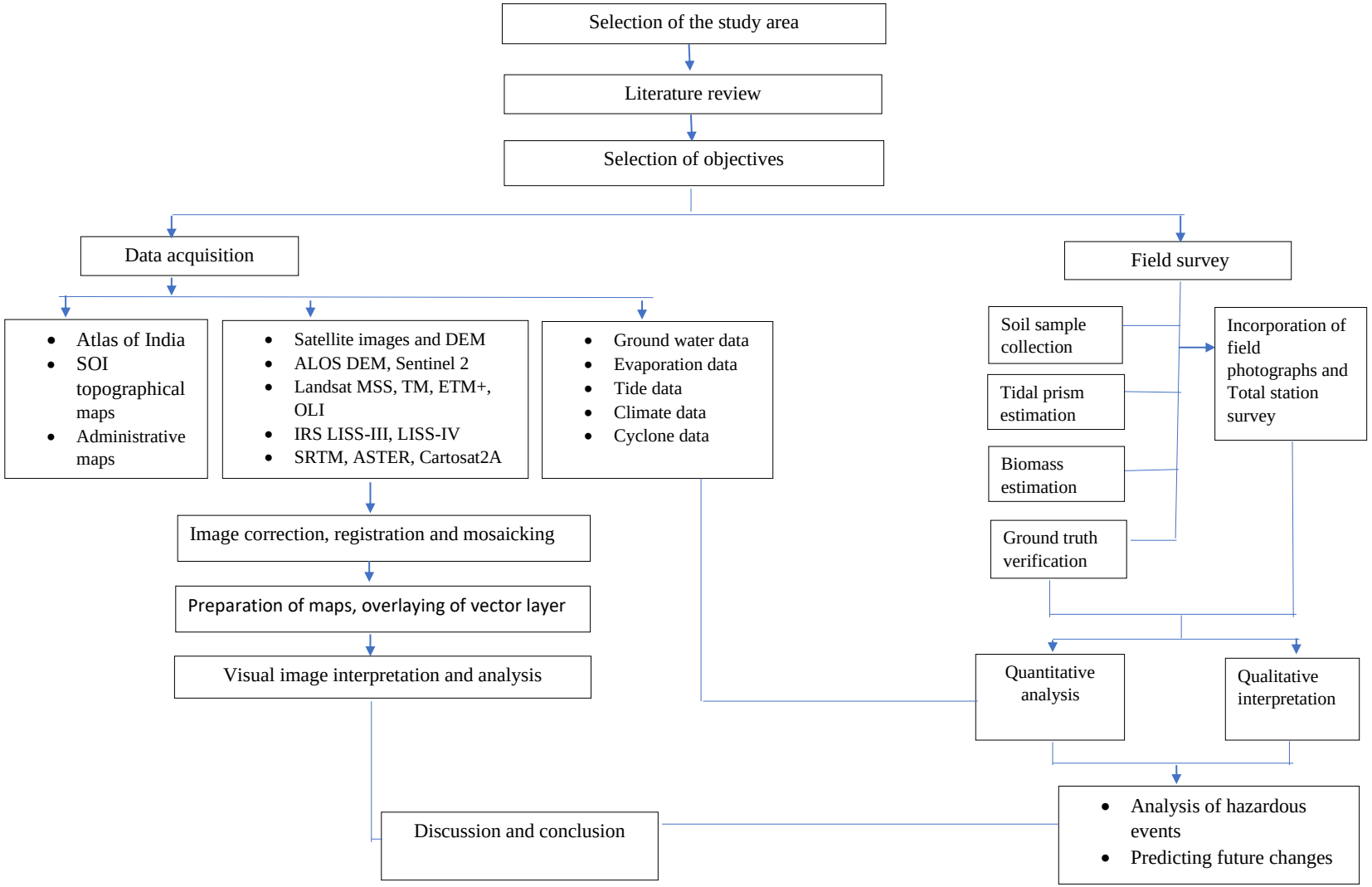

Figure 1.18: Flowchart of the methodology of the research work.

were collected from Port Trust office. Open series toposheets and District Planning Map Series of South 24 Parganas were collected from Survey of India and NATMO. Climate data(2000-2020) 20 years were collected from Indian Meteorological Department. Ground water data for South 24 Parganas were obtained from Centre for Ground Water Study. Evaporation data was collected from Indian Council of Agricultural Research (ICAR) for 2000-2020. All the Satellites and ALOS PULSAR DEM, SENTINEL IMAGE, SRTM, ASTER DEM were downloaded from BHUVAN and USGS platform in three seasons. Cartosat 2A DEM was purchased from National Remote Sensing Centre (NRSC).

To monitor the seasonal changes of saltpans and their soil characters, vegetation characteristics of the islands, field survey in pre-monsoon, monsoon, post-monsoon were out in each year. Sediment sample collection from 15 locations within islands in three seasons, water sample collection from pond and tube wells, topographic survey with total station, beach profiling with transit theodolite and dumpy level were carried out. Apart from these slope measurements done with clinometers, height of the mangroves was measured by abneys level. Biomass estimation, tidal prism estimation was done in both Henry's and Patibania islands in three years. Pore water salinity also measured by pore water sucker. Ground truth verification was carried out by Global positioning system (GPS). Questionnaire survey, and collection of field photographs also a integral part of field survey.

In post-field survey all the sediment samples are analyzed in laboratory. 12 soil parameters were tested from each sample. Compilation and plotting of primary data through statistical software were done. Several maps were prepared based on DEM and Satellite images. Image interpretation, qualitative and quantitative analysis, trend analysis were done through proper statistical techniques. Impact assessment were tried to establish along with a hydrological model with proper management process. In Figure 1.18, the flowchart of the methodology adopted in the current work is presented.

1.10.1 Materials used

In this section, the materials and the data sources that were used in the research work are described.

- Collection of Topographical maps (Nos-F45Q2, F45Q6) Open Map Series, Scale-1:50,000 from Survey of India (SOI)

- District Planning Map Series of South 24 Parganas and another topographical sheet 79C (Scale-1:250,000) were acquired from NATMO.
- Use of ALOS DEM (12.5m resolution) from NASA Earth Data for topographical mapping and Cartosat 2 DEM (1m) was procured from National Remote Sensing Centre(NRSC) for identification of geomorphic settings of the islands.
- Selected Satellite Database LANDSAT 5(TM) for 2000, LANDSAT 7 ETM+ for 2010 and LANDSAT 8 OLI/TIR for 2020 downloaded from USGS and BHUVAN platform for mapping of Salinity Index, MAVI and Bareness Index for both the islands.
- Sentinel 2 image collected from USGS website for Biomass mapping of the islands.
- Evaporation (2000-2019) data of Canning station was collected from Indian Council of Agricultural Research (ICAR) and Rainfall, Relative Humidity, Temperature(2000-2020) of the station Diamond Harbour was purchased from Indian Meteorological Department (IMD) for the climate trend analysis over the study area.
- Ground water data of Bakkhali was collected from Central Ground Water Board (CGWB).
- Hooghly river tide table (2018) was purchased for the station Diamond Harbour, from Port trust to assess the tidal fluctuations over the islands.
- Cyclone data was collected from IMD website to get the information of the occurrence of cyclones in last 20 years.

Next, in Table 1.3, detailed description of the field work is provided, including the places visited, the dates, the purpose of visit, the instruments used to collect data and conduct experiments and the techniques followed.

Table 1.3: Detailed field work description

Fieldwork (Place visited)	Date	Purpose of visit	Instrument used	Techniques followed
Henry's island	08.09.2014	Ground truth verification and observation of saltpans.	• Garmin eTrex GPS receiver • Canon PowerShot A2100 camera	Identification of saltpans and sediment collection from different saltpans.
Henry's island and Patibania island	12.4.2015 to 15.4.2015	Sediment sampling from different geomorphic settings	• Garmin eTrex GPS receiver • Canon PowerShot A2100 camera	Soils were collected from 15 location of saltpan based on elevation and mangrove characters.

Henry's island	18.8.2015 to 22.8.2015	Monitoring of soil character, soil sample collection.	• Garmin eTrex GPS receiver • Canon PowerShot A2100 camera	Soil sample collection from mangrove habitats.
Henry's island and Patibania island	23.12.2015 to 27.12.2015	Litho pit cutting of soil and water quality analysis.	• Garmin eTrex GPS receiver • Canon PowerShot A2100 camera • Refractometer • BOD meter	Stratigraphical measurement of soil. Sediment collection from different location within islands. Water quality assessment from salt ponds and tube well with BOD meter and refractometer for alkalinity measurement.
Henry's island and Patibania island	05.05.2018 to 09.05.2018	Sediment collection, topographical survey of saltpans.	• Garmin eTrex GPS receiver • Canon PowerShot A2100 camera • Leica TC–805 Total Station	Contour map preparation with the help of total station.
Henry's island and Patibania island	20.09.2018 to 25.09.2018	Sediment collection, slope measurement.	• Garmin eTrex GPS receiver • Canon PowerShot A2100 camera • Clinometer • Measuring tape	Slope measurement of beach and saltpan area with clinometers. Sediment collection.
Henry's island and Patibania island	23.01.2019 to 26.01.2019	Topographical survey, soil sample collection, biomass estimation, tidal prism estimation.	• Garmin eTrex GPS receiver • Canon PowerShot A2100 camera • Leica TC–805 Total Station • Biomass sampling quadrant (2m/2m) • Weight machine • Measuring tape • Ranging rod • Abneys level	Above ground biomass estimated. Height of the large, medium, small and very small trees were measured by abney's level. Measurements of creeks and velocity of tidal water were measured by current velocity meter. Long and cross profile of the creeks were done.
Henry's island	06.05.2019 to 09.05.2019	Beach profile, pore water salinity measurement.	• Garmin eTrex GPS receiver • Canon PowerShot A2100 camera • Dumpy level • Pore water sucker	Elevation profile were carried out in Kiran beach of Henry's island with Dumpy level. Pore water was collected and kept in the measuring bottle. Soil samples also collected.

Henry's island and Patibania island	10.10.2019 to 15.10.2019	Measuring of Crab holes for bioturbation estimation.	• Garmin eTrex GPS receiver • Canon PowerShot A2100 camera • 1m/1m measuring quatrant • Measuring tape • Dumpy level	Diameter and depth of crab holes were measured in saltpan and beach area. Distance from the smaller crab holes to medium and large were measured by tape. Soil samples were collected along the burrows and elevation value was measured.
Henry's island	12.01.2020 to 15.01.2020	Identification of mangrove succession, soil sample collection, observation of sedimentary structure.	• Garmin eTrex GPS receiver • Canon PowerShot A2100 camera	Photographs were taken on different ripple marks on beach. Soils sample were collected. Three succession level of mangroves identified from beach to inland. Including within saltpans.

1.11 Methodology

In this section, the methodology adopted for the analysis of collected data is described.

1.11.1 Analysis of DEM and images

For the assessment of topography, micro-contour zonation map are prepared on the basin of Cartosat2 DEM whose resolution is 1 m using the ARC GIS (10.1) software. Firstly, the area of interest, i.e., the Henry's island and the Patibania island are clipped using clip option of raster processing tool from arc toolbox in ARC GIS software. With the help of spatial analyst tool, isopleths are generated with 0.22 m interval in both the islands. Geomorphic settings of the islands are clearly identified from this micro-zonation of topography. Next, for tidal inundation map preparation, Google earth Pro for 2016 is used. For the assessment of tidal inundation level in pre-monsoon, monsoon and post-monsoon (January, March and September) months are taken. Then on the basis of daily tidal data and time of occurrence in Bay of Bengal, frequency of tidal inundation in a month is prepared in MS EXCEL. After that, isolines are drawn on Google Earth satellite image on the basis of frequencies of tides and elevation of topography. On Cartosat-2A Dem (1 m resolution) where saltpatches are identified and vector layers are generated by digitization techniques in both islands to prepare a saltpan identification map.

For the geomorphic classification of the study areas Shuttle Radar Topographic Mission (SRTM) downloaded from USGS are used, eighteen geomorphic settings in Henry's island and eleven geomorphic settings in Patibania island have been identified. By the process of vector layer creation these maps are prepared in ARC GIS software. To estimate vegetation canopy biophysical properties of the islands, normalized difference vegetation index (NDVI) maps are prepared on Landsat 8 OLI/TIRS C1 Level1 (spatial resolution 30 m) images for 2005, 2010, 2015, 2019. For this maps, NDVI formula used NDVI=NIR-R/NIR+R (Huete and Liu, 1994; Leprieur et al., 2000). Here N and R represents surface reflectance average over visible ($\lambda \sim 0.6$ Î¼m) and NIR (($\lambda \sim 0.8$ μm) regions of spectrum. NDVI is related to leaf area index (LAI) and vegetation condition and biomass. To estimate detailed LAI of the vegetation and vegetation condition within different background condition, moisture adjusted vegetation index (MAVI) (Zhu et al., 2014) has been prepared. Red, near infrared, and shortwave infrared (SWIR) reflectance in band-ratio form are considered in this estimation. Formula used for MAVI calculation is MAVI = (NIR-R)/(NIR+R+SWIR) (Zhu et al., 2014). Here R represents red, NIR represents near infrared and SWIR represents short wave infrared bands. MAVI has higher sensitivity to LAI then NDVI. MAVI maps have been prepared for the year 2000, 2010, 2020. In case of 2000 and 2010 Landsat 5 TM C1 Level -1 is used, for 2020 Landsat 8 OLI/TIRS C1 Level 1 is applied. Apart from these, Moisture index (MI) and Normalized Difference Salinity Index (NDSI) for the same years have been prepared in ARC GIS (10.1) software. The following formula has been adopted for MI: MI = LSTmax- LST / LSTmax-LSTmin, where LSTmax = a1 * NDVI + b1, LSTmin = a2 * NDVI + b2, LSTmax and LSTmin being the maximum and the minimum surface temperature for a given NDVI, and LST being the remotely sensed data derived from surface temperature at a given pixel for a given NDVI (Polpanich et al., 2002).

To compare the changes in the area of saltpans in the different years, supervised classification techniques are used on Landsat 5TM C1 Level1 for 2000, Landsat 7 ETM + C1 Level -1 for 2010 and Landsat 8 OLI/TIRS C1 Level 1 for 2020. TNTmips software is used for supervised classification using maximum likelihood classifier for delineation of saltpans in three consecutive years. For habitat mapping for both the islands, unsupervised classification techniques are applied with the help of isodata classification algorithm in TNTmips software. In this case, Google Earth Satellite image is used (quick bird of 2018 has been used as a base map for this mapping of both island. Drainage map has prepared in QGIS (3.10) software with

vector layer creation and their area also are calculated in raster calculator. ALOS PALSAR DEM (12.5 m resolution) is used for the inundation map of Amphan supercylone surge. Alaska Satellite facility archive is used for downloading the data. After that, radiometric correction has done in ARC GIS software and final inundation map has been prepared. Shore line erosion and deposition mapping was done on Google Earth quick bird images for 1990, 2000, 2010 and 2020. First,vectors layers were created, then they were overlapped to estimate the rate of erosion and deposition in QGIS (3.10) software.

1.11.2 Soil data analysis

Soil samples, which were collected from field survey in pre-monsoon, monsoon and post-monsoon seasons in different years at 15 locations in the islands, are analyzed in a soil laboratory. Each soil sample was chemically analyzed, and the quantities of the following twelve variables were measured: soil pH, electrical conductivity, the percentages of moisture, sand, silt and clay, the salinity, the soil organic carbon and the soil organic matter, the available nitrogen, phosphorus and potassium. Total 94 soil samples were collected and 12 parameters are analyzed for each sample, which means total 1128 measurements were recorded from soil analysis. This data are statistically analyzed using R software and MS EXCEL. For the assessment of sedimentary structure and bioturbation analysis, 50 samples were collected from the different sedimentary structures of the Kiran beach and the Bakkhali beach along the crab holes and animal burrows. Textural analysis was done in soil laboratory with the sieving techniques. Sieve numbers 14, 18, 35, 60, 120, 170, 200, 230 and pan were used. 100 gm weight of each sample was weighted and then kept for air drying. Subsequently, they were oven dried and finally measured. These data were statistically analyzed in the gradistat software for mean, standard deviation, skewness and kurtosis values. Mud analysis was done for the sample of bioturbation structure with hydrometer analysis in soil lab. 50 gm soil samples were taken from each sample, which were air dried after coning and quartering. Then 5% solution of Sodium Hexaphosphate was prepared. 50% O NaPO3 solution was added to the sample and then stirred vigorously with the dispersing machine for 15-20 minutes. After that, 880 ml de-ionized water was added to the sample and shaken for 25-30 minutes before taking the reading. Next step was adding 3 drops of isoamyl alcohol to the solution and then starting a stop watch and put the cylinder on a stable place. Then, 3-5 times readings were taken at 40 sec using soil hydrometer ASTM 152h. Reading of soil temperature was also taken by thermometer. After 2 hrs interval, again reading was taken.

Finally a blank solution was taken and a reading was taken at the starting and ending time by soil hydrometer and thermometer.

Plate 1.1: Photographic evidence of field survey.

1.11.3 Field analysis

Repeated field monitoring was carried out in three seasons per year over 5 years. Soil samples were collected from different geomorphic settings of the two islands aided by GPS and camera. Field photographs are taken to record the geomorphic settings. Firstly, geomorphic settings identification was done aided by GPS. After that, Total Station was used for the analysis of topographic characters in saltpans. Beach profiles were taken with Dumpy level at 2 m interval, covering full Bakkhali beach and Kiran beach. Long and cross profiles were recorded for the large, the medium and the small creeks for tidal behavior estimation. Pore water salinity was estimated by sucker. Soil temperature, alkalinity, salinity was also measured. Slope measurements was done by clinometer. Above ground biomass was estimated with 5m/5m quadrant method, measuring tape and weight machine.

Identification of measurements of sedimentary structures like ripple marks along the shoreline were carried out before and after high tides. Identification of bioturbation structures was done at beaches and saltpans in three seasons with proper field photographs and measuring equipment. Observation of changing soil characters specially in pre-monsoon, monsoon and post-monsoon within saltpans was made. Succession pattern of mangroves from sea beach to inner parts of the islands were noted. Estimation of drainage characters of the islands was done. Changing mangrove characteristics within saltpan in three seasons was studied. Questionnaire survey to the tourists in three seasons at the Henry's islands was carried out. Estimation of ground water level in both islands, specially in the pre-monsoon season, was done. In Plate 1.1, some photos taken during the field investigation are presented.

1.11.4 Statistical analysis

In this subsection, the statistical methods employed to analyze the collected data are described. The statistical analysis is divided in three parts: the analysis of the 12 soil variables, the trend analysis of the climate components and the seasonal hydrological balance of the two islands and its temporal change.

Analysis of soil variables

The means and the standard deviations of the 12 soil variables are computed over the seasons in the islands. From this, the changes in the means and the standard deviations over the seasons

are investigated. To further investigate the changes in the distributions of the soil variables over the seasons in the islands, comparative boxplot analysis and density plots are also used.

The boxplot provides information about the center, the spread and the skewness of the sample as well as the presence of outliers. The comparative boxplot analysis yields information about the change in the median levels of the soil variables over the seasons, and also conveys the changes in the dispersion and the skewness of the variables. However, boxplots only provide limited information about the shape of the underlying distribution, and cannot provide any information about multi-modality. For this reason,the datasets are also analyzed using their estimated densities. The densities are estimated using Gaussian kernels.

The boxplots and the density plots provide visual indication of differences among the groups. However, to ascertain whether the differences are statistically significant or not, analysis of variance (ANOVA) was carried out in the datasets. The ANOVA tests whether there is a statistically significant difference among the means of the classes. A small p-value for the ANOVA test implies statistically significant difference among the group means. For example, if the p-value of the ANOVA test is smaller than 5%, one can state that there is a statistically significant difference among the group-means at 5% level. One may also consider other levels, e.g., 1%, to reject the null hypothesis (the ANOVA null hypothesis is that all the group-means are identical, so rejecting the null hypothesis means stating that there is a statistically significant difference among the group-means). Here, the level is taken as 5%.

The ANOVA procedure assumes that the observations follow normal distributions with equal variance (homoscedasticity). These two assumptions, i.e., that the observations are normally distributed and homogeneity of variances, may not hold in practice. To check whether the assumptions are satisfied in the concerned data, the Shapiro-Wilk test of normality (Shapiro and Wilk, 1965; Royston, 1982b,a, 1995) and Levene's test for homogeneity of variance across groups (Levene, 1960) are used. A small p-value of the Shapiro-Wilk test indicates towards the non-normality of the data, while a small p-value of Levene's test points toward the heterogeneity of variances among the groups (heteroscedasticity). If the p-value of the Shapiro-Wilk test is smaller than 5%, it implies that there is a statistically significant evidence of non-normality of the distributions of the groups at 5% level. If the p-value of the Levene's test is smaller than 5%, one can state that the distributions of the groups are heteroscedastic in nature at 5% level.

Under non-normality or heteroscedasticity, the ANOVA procedure does not work satisfactorily to discern the difference among the group means. In that case, the Kruskal-Wallis test

(Kruskal and Wallis, 1952) may be used. This test checks whether the underlying distributions of all the groups are the same. A small p-value indicates that the distributions of the groups are different. So, a p-value of the Kruskal-Wallis test smaller than 5% implies that there is a statistically significant difference among the underlying distributions of the groups at 5% level. The Kruskal-Wallis testing procedure only requires the independence of the observations for its validity, which is far weaker requirement than the ANOVA procedure. In particular, it does not require normality of the underlying distributions of the groups nor homoscedasticity. However, if the data actually satisfy normality and homoscedasticity, then the ANOVA procedure is more powerful than the Kruskal-Wallis test. For the analysis of the datasets, both the ANOVA procedure and the Kruskal-Wallis test are carried out.

In case the ANOVA or the Kruskal-Wallis test yields a small p-value lower than a certain level, which indicates a statistically significant difference among the group-means or the distributions of the groups, respectively, one may be interested exactly which pairs of group-means or which pairs of group-distributions have a statistically significant difference. For this, the Tukey honest significant differences test is employed, which is also known as Tukey's range test (Tukey, 1949) to compare the group-means. In addition, the pairwise Wilcoxon rank sum test (Wilcoxon, 1945) along with the Benjamini-Hochberg procedure to adjust p-values for multiple testing (Benjamini and Hochberg, 1995) is used to compare the pairs of the distributions of the groups. If the p-value of the Tukey honest significant differences test for a particular pair of group-means is small, it indicates that the particular pair of group-means are statistically different. For example, if the p-value of the Tukey honest significant differences test is less than 5%, one can state that there is a statistically significant difference between the two group-means at 5% level. Similarly, if the p-value of the pairwise Wilcoxon rank sum test for a particular pair of groups is less than 5%, one can state that there is a statistically significant difference between the distributions of the two groups at 5% level.

Next, the pairwise association of the soil variables is analyzed. For this, the Pearson product-moment correlation coefficient, the Spearman's rank correlation coefficient and the Kendall rank correlation coefficient are used along with their associated tests to check if the correlation is statistically significant or not.

Let $(X_1, Y_1), \ldots, (X_n, Y_n)$ be the paired sample, and let $\bar{X} = n^{-1} \sum_{i=1}^{n} X_i$ and $\bar{Y} =$

$n^{-1}\sum_{i=1}^{n} Y_i$. The Pearson product-moment correlation coefficient is defined as

$$\rho_{X,Y} = \frac{\sum_{i=1}^{n}\left(X_i - \bar{X}\right)\left(Y_i - \bar{Y}\right)}{\sqrt{\sum_{i=1}^{n}\left(X_i - \bar{X}\right)^2}\sqrt{\sum_{i=1}^{n}\left(Y_i - \bar{Y}\right)^2}}.$$

The Pearson product-moment correlation coefficient lies between 1 and -1, and it measures the strength of linear association between the variables. The Pearson correlation is 1 when there is a perfect positive linear association between X_i's and Y_i's, i.e., $Y_i = a + bX_i$ for all i, where b is a positive number and a is any number. On the other hand, the Pearson correlation is -1 when there is a perfect negative linear association between X_i's and Y_i's, i.e., $Y_i = a - bX_i$ for all i, where b is a positive number and a is any number like before.

To visually present the correlation structure of the variables, correlation plots are employed for all three correlation coefficients. In the correlation plots, the statistically significant (at 5% level) correlation values have colored background. The darkness of the background color increases as the absolute value of the correlation increases. Positive correlations and negative correlations have different colors.

Trend analysis of climate

Climate plays a paramount role in shaping the distribution of mangroves and also the geomorphology of the coastal areas. Climate data were collected on five variables: maximum temperature, minimum temperature, rainfall, evaporation, relative humidity measured in the morning and in the evening. Daily record on this five variables over the 20 years period from from 2000 to 2019 were collected. From these data, fortnightly, monthly, seasonally and yearly trends of the climate variables are analyzed. Because the two islands, are so close to each other, they experience the same climate and it is not required to analyze the climate of two islands separately.

Apart from the five primary climate variables, another quantity related to the climate is analyzed, which is the potential evapotranspiration. The potential evapotranspiration is mainly determined from the temperature. The estimated potential evapotranspiration using Thornthwaite's method (Thornthwaite, 1948) for a month m is defined by the following:

$$PET_m = 16\left(\frac{L_m}{12}\right)\left(\frac{N_m}{30}\right)\left(\frac{10T_m}{I}\right)^{\alpha},$$

where

- PET_m is the estimated potential evapotranspiration (mm/month) of the month m,

- L_m is the average day length (hours) of the month m,
- N_m is the number of days in the month m,
- T_m is the average temperature (degrees Celsius) of the month m, if that is positive, else T_m is taken as 0,
- I is a heat index defined by

$$I = \sum_{i=1}^{12} \left(\frac{T_{m_i}}{5} \right)^{1.514},$$

  where T_{m_i}'s are the average temperatures of the 12 months in a year,
- and α is defined as

$$\alpha = \left(6.75 \times 10^{-7}\right) I^3 - \left(7.71 \times 10^{-5}\right) I^2 + \left(1.792 \times 10^{-2}\right) I + 0.49239.$$

Note that given the average temperatures of the 12 months, one can calculate all the estimated monthly PET values of the year. In the case under consideration, the average maximum temperatures and the average minimum temperatures of all the months are available. The average temperature of a month is estimated by taking the average of the average maximum temperature and the average minimum temperature of that month. After the estimation of the monthly potential evapotranspiration, trend analysis is carried out.

Regression analysis of the inter-relationship of saltpans, mangroves, climate and soil characteristics

There is close relationship among the saltpans, the mangroves, climate variables and the soil characteristics. With the objective f studying these inter-relationships, the total area of the saltpans in both the islands are acquired from remote sensing data over several years. From the NDVI data, the area under dense mangroves, moderate mangroves and mangroves of low density are calculated over the years. The yearly levels of the five climate variables for the same years were taken. Finally, the yearly average levels of the 12 soil variables were considered. Taking all these variables over the years, linear regression analysis was carried out taking two of the variables at a time, with each of the variables from a different set. For example, the regression analysis involves a mangrove variable and a soil variable, but not two soil variables as they are from the same set. For each pair of variables, two linear regressions are carried out by swapping

the response and the covariate. However, a climate variable is only considered as a covariate and never as a response, as variables related to saltpans, mangroves and soil characteristics cannot influence the climate variables. This pairwise linear regression analysis yields insight into the inter-dependence of the saltpans, the mangroves and the soil characteristics and how these are influenced by the climate.

Hydrological balance of the islands

The hydrological balance of the two islands are estimated with the objective to study the balance of fresh water and saline water in these two islands. The components of the hydrological balance in the Henry's island and the Patibania island are estimated for the years 2010 and 2019. Each of the two years are divided in three seasons: pre-monsoon, monsoon and post-monsoon, and the components are estimated seasonally. The reason for considering this particular division of seasons is that the monsoon rainfall plays an important role in the climate. For a year, the pre-monsoon season is considered from February 15 to June 14 of that year, the monsoon season from June 15 to October 15 of that year, and the post-monsoon season is considered from October 16 of that year to February 14 of the next year. So, in a year with 365 days, the pre-monsoon season has 120 days, the monsoon season has 123 days, and the post-monsoon season has 122 days. Here, the components and the methods of their estimation are described.

The hydrological balance has two categories of components: source and consumption. The source is again divided into source of freshwater and source of saline water, since the main objective is to investigate the balance of freshwater and saline water and its variation over the seasons. Consumption is divided into natural consumption and artificial consumption. Natural consumption is consumption of water in various geological and climatic processes. Artificial consumption means in this context the anthropogenic consumption and the consumption by local fauna in the respective islands. Some of the consumption components correspond to the consumption of exclusively freshwater, and the rest correspond to the consumption of both freshwater and saline water.

Sources of freshwater are two: rainwater and drawing from groundwater. Sources of saline water are three: tidal inundation in the islands, tidal prism in the creeks in the respective islands, and storm surges resulting from the occasional cyclones. The water consumption activities included in artificial consumption use utilize freshwater exclusively, as human activities consume only freshwater, and the local fauna also consume only freshwater. Natural consumption consists

of surface runoff, channel runoff, throughflow, evaporation and ground water recharge. Surface runoff is the outflow of rainwater that is not absorbed through the surface. So, surface runoff consumes only freshwater. Channel runoff is considered as the combined outflow of rainwater and saline water through the creeks in the islands. Throughflow is the subsurface outflow from the islands to the creeks. Its sources are both rainwater and saline water. Evaporation consumes both rainwater and saline water in the islands. Ground water recharge also happens from both rainwater and saline water. Hence, within natural consumption, surface runoff consumes exclusively freshwater, while channel runoff, throughflow, evaporation and ground water recharge consume both freshwater and saline water. Below, the estimation procedure of each of the components is described in the section.

Rainwater: Daily rainfall data is available over the years in mm in the region encompassing the islands. The total seasonal rainfall heights in mm are obtained for the three seasons by summing the respective daily rainfall heights. For example, to get the total rainfall height in mm corresponding to pre-monsoon in 2010, the daily rainfall heights in mm are summed from February 15, 2010 to June 14, 2010. Next, from the seasonal total rainfall heights, the seasonal total rainfall volumes in cubic meters are calculated. This is done by converting the rainfall heights to meters and the island area to square meters, and then multiplying them. Recall that rainwater is one if the two sources of freshwater in the islands.

Evaporation: The estimation procedure of evaporation is identical to that of rainfall volume. The daily evaporation data in mm are available in the years 2010 and 2019. Then seasonal total evaporation heights are calculated from the daily data like in the case of rainfall heights. The seasonal total evaporation heights are converted from mm to meter, and these values are multiplied by the areas of the islands in square meters to estimate the seasonal total evaporation volumes in cubic meters.

Groundwater: Note that groundwater is present as both source and consumption in the hydrological model. Data on the depth of the groundwater table from the surface in the region encompassing the two islands were obtained. When one finds that the groundwater table has fallen in a season, it can be concluded that water was drawn from the groundwater table, and hence in that season groundwater acts as a source. Also note that groundwater is part of freshwater. So, in the particular season where the groundwater table falls, groundwater acts a source of freshwater. In seasons, when the groundwater table rises, it can be concluded that water is absorbed in recharging groundwater. Since groundwater recharge occurs from both

freshwater and saline water, in the seasons when the groundwater table rises, groundwater acts as a consumption point of both fresh water and saline water combined. It is assumed that the values of the depth of the groundwater table correspond to the depth of the groundwater table at the end of the corresponding season, so that the effect of the full season is reflected there. The volume in cubic meters of groundwater used as freshwater in a particular island is estimated by multiplying the increment in the depth in meters of the groundwater table by the area of the island in square meters. If it is found that the depth of the groundwater table decreased in a season compared to the preceding season, this means there was a recharge of groundwater from freshwater and saline water available in that season. To estimate the volume of combined fresh water and saline water used to recharge groundwater in the season in a particular island, the decrease in the depth of the groundwater table is multiplied by the area of the island.

Tidal inundation: A high tide inundates a portion of the island area by saline water. This way, the volume of saline water involved in the inundation of the island area serves as a source of saline water in the island. Tides occur in pairs: a high tide is followed by a low tide, and vice versa. Data on the height in meters of water from the river bottom during high tides and low tides were obtained. The height of the mean water level from the bottom of the river is the average of the height at a high tide and the height at the corresponding low tide. This mean height is subtracted from the corresponding heights at the high tide and the low tide for every pair of high tide and low tide. The height values obtained by subtracting the mean height from the corresponding heights of the high tide and the low tide are called 'centered' heights, since the mean height value lies at the middle of the heights at the high tide and the low tide. So, all the centered height values for the high tides are positive and the centered height values for the low tides are negative. By subtracting the mean height values from the corresponding height values at high tides and low tides, the effect of the particular location where the heights were measured from the bottom of the river is eliminated.

Next, the procedure using which the tidal inundation volume at the islands during the high tides are estimated is described. The area of each of the islands is divided in zones according to its elevation in meter from the mean sea surface. Each zone has its corresponding maximum elevation and minimum elevation. Also note that the centered height of a high tide is the height of water in the surrounding creeks and the sea from the mean sea surface level during the high tide in an island. So, one can compare the centered heights of the tides to the elevations of the regions in the islands, which are also measured from the mean sea surface level, to get the

inundated region.

To estimate the volume of saline water brought to the island through tidal inundation, the estimated volume of saline water present in the completely inundated zones is added to the estimated volume of saline water present in the partially inundated zone. Due to the nature of the elevation based classification of zones, there can be several completely inundated zones, but there can be at most one partially inundated zone.

To estimate the volume of saline water present in a completely inundated zone in cubic meters, the average height of the water column over that zone in meters is multiplied with the area of that zone in square meters. The average height of the water column over a completely inundated zone is estimated by subtracting the average elevation of that zone from the centered height of the high tide under consideration. And the average elevation of that zone is estimated by taking the average of its maximum elevation and minimum elevation.

Next, to estimate the volume of saline water present in a partially inundated zone, first the inundated area in that zone is estimated. For this, the maximum height of the water column in that zone is computed, which is obtained by subtracting the minimum elevation from the centered height of the high tide under consideration. The inundated area in the partially inundated zone is estimated by multiplying the total area of that zone by the ratio of the maximum height of the water column in that zone to the difference of the maximum and the minimum elevations in that zone. This method of estimating the inundated area assumes that there is a linear relationship between the elevation value and the area under the elevation value in the zone. That is, if the elevation is denoted as y and the area in that zone under elevation y is denoted as x, then it is assumed that $y = a + bx$ for some $b > 0$ and some number a. The estimated value of the inundated area thus obtained would be close to the actual value if the elevation varies gradually over the zone, and there is no sudden change in elevation. This is generally true for such low lying area in a river delta. Next, the average height of the water column in the partially inundated region in that zone is estimated by half the value of the maximum height of the water column in that zone. This is because actually the average height of the water column in the partially inundated region of that zone is estimated by the average of the maximum and the minimum heights of the water column in that partially inundated region, and the minimum height of the water column in a partially inundated region is 0. So, the average of the maximum and the minimum heights of the water column in that partially inundated region is equal to half the value of the maximum height of the water column there. Finally, the volume of saline water present

in a partially inundated zone is estimated by the product of the estimated inundated area in that zone and the estimated average height of the water column in the partially inundated region of that zone.

Using the method described above, the volume of saline water available through tidal inundation corresponding to each of the high tides in the year is estimated in the two islands. Based on the time of occurrence recorded for each of these tides and the estimated volume of saline water brought to the islands through tidal inundation corresponding to each of the high tides, the daily tidal inundation volume is estimated for each day of the year by adding the estimated volume of saline water brought to that island through tidal inundation corresponding to the high tides which occurred on that day.

From the estimated daily tidal inundation volumes in an island, the seasonal tidal inundation volumes in that island for the three seasons is estimated by summing the values of the daily tidal inundation volume corresponding to the dates which constitute that particular season. For example, to estimate the pre-monsoon seasonal tidal inundation volume in Henry island, one sums the estimated daily tidal inundation volumes in Henry island from February 15 to June 14, as the duration from February 15 to June 14 constitutes the pre-monsoon season.

The computation related to the estimation of the tidal inundation volumes are carried out in R.

Tidal prism: Tidal prism is the volume of saline water brought into the creeks of an island during a tide cycle, which consists of a low tide and its corresponding high tide. So, it is a source of saline water in the islands. It is estimated by the product of the tidal range and the surface area of the basin. The tidal range of a pair of high tide and a low tide is the difference of the tidal heights. The surface area of the basin is estimated by the product of the length of the creek and its average width.

Each of the islands has several creeks. To estimate the tidal prism associated with a particular tide cycle in an island, the estimated tidal prisms associated with that tide cycle in all the creeks of that island are added. the creeks in the two islands are described below.

The creeks in the Henry's island are divided in three categories based on their sizes: large, medium and small. There is one large creek, two medium creeks and four small creeks. It is assumed that the sizes of the creeks within each category are identical. The widths of a creek were measured at two cross sections: one at the beginning of that creek and the other at the end of that creek, and the average width of that creek is taken as the average of these two width

values. The creeks in the Patibania island are also divided in three categories based on their sizes: large, medium and small. There is one large creek, one medium creek and three small creeks in the Patibania island, and it is again assumed that the sizes of the creeks within each category are identical. Like in Henry island, the widths of a creek were measured at two cross sections: one at the beginning of that creek and the other at the end of that creek. The average width of a creek is taken as being equal to the average of its width at the two cross section. The lengths of each type of creeks were measured. The lengths of each type of creeks were measured in both the islands.

From the daily tidal prism values in an island, the seasonal tidal prism in that island for each of the three seasons is estimated by summing the daily tidal prism values corresponding to the dates which constitute that particular season.

The calculation for the tidal prism estimation was carried out in R.

Cyclone surge: The storm surges associated with cyclone in Sundarbans inundates the islands with saline water. This way, the cyclone surge act as a source of saline water in the islands. Record of the heights of the storm surges from the mean sea level in meters were acquired along with the dates of their occurrence. From these heights and the elevation profiles of the islands, the volume of saline water brought to each of the islands by the cyclone surges is estimated in the same way as in the case of tidal inundation. Here, it is not needed to center the cyclone surge heights like in the case on tidal heights in tidal inundation estimation, because the cyclone surge heights were measured from the mean sea level. Based on the dates of occurrence of the cyclone surges, they are classified into the three seasons. To estimate the seasonal volume of saline water from cyclone surges, the volumes of saline water from the storm surges occurring in that particular season are added.

Like tidal inundation and tidal prism, the computations related to estimating the volume of saline water from cyclone surges is also carried out in R.

Surface runoff: During and after rainfall, the volume of rainwater that is not absorbed in the soil flows of as surface runoff. Thus, surface runoff consumes freshwater. The volume of surface runoff is estimated by multiplying the volume of rainfall by a surface runoff coefficient. The runoff coefficient for a forested mangrove region is taken as 0.3.

Channel runoff: Channel runoff is the amount of water flown from an island into its adjacent creeks. It consumes both freshwater and saline water. Recall that measurements from each type of creeks were taken at two cross sections: at the beginning or upstream of the creek, i.e., where

the creek enters the island, and at the end or downstream of the creek where it leaves the island. Apart from the width in meters, the depth of water in the creek was also measured in meters at the two cross sections. In addition, the velocity of water entering at the upstream cross section and the velocity of water leaving the downstream cross section were measured for each type of creeks. Data on velocity of water, width of the cross sections and average depth of water there were collected only once for each type of creeks.

By multiplying the width and the average depth of a cross section, the estimated area of that cross section is obtained. By multiplying the estimated area of a cross section with the velocity of water passing through that cross section, the volumetric flow rate of water passing through that cross is obtained. Finally, by subtracting the volumetric flow rate at the upstream cross section of a creek from the volumetric flow rate at the downstream cross section, the volume of water flowing to that creek from the island per second is obtained. By multiplying this subtracted value of a creek with the total number of creeks of its type, the volume of water flowing from the island to the creeks of that particular type per second is estimated. Next, the volumes of water flowing from the island per second to the creeks of all types are added, and then by multiplying this sum by the number of seconds in a day, the estimated daily channel runoff in that island is obtained. Finally, the seasonal channel runoff in a particular island is estimated by multiplying the estimated daily channel runoff in that island by the number of days in that season, e.g., pre-monsoon has 120 days, monsoon has 123 days and post-monsoon has 122 days.

Throughflow: Throughflow is the subsurface flow of water from an island to its adjacent creeks or the sea. Throughflow consumes both freshwater and saline water. To estimate throughflow, one measurement was taken at a place in the mangroves in the Henry's island on the banks of a creek. There, an empty bottle of volume 500 ml was placed subsurface for 45 minutes to measure how much of that bottle gets filled up with water from the soil. It was found after 45 minutes that 150 ml water was there in that bottle. Since the source of this water was throughflow, this measurement is used to estimate it. First, by dividing the volume of 150 ml by the number of seconds in 45 minutes, the volumetric flow rate is obtained, which is 0.056 ml/s. It is assumed that this volumetric flow rate presents the throughflow rate from one square meter of surface containing mangroves in the island. However, this measurement was taken in the mangroves, but the island also contains nonmangrove regions and bare surface. So, the throughflow rates on non-mangrove and bare surfaces are estimated by multiplying the

throughflow rate of mangrove by 0.7 and 0.5, respectively. Based on the above, the throughflow rate of mangrove is 0.056 ml/(s m^2), that for nonmangrove is $(0.056 \times 0.7) = 0.0392$ ml/(s m^2), and for bare surface it is $(0.056 \times 0.5) = 0.028$ ml/(s m^2).

The the total area of mangrove covered regions, the total area of nonmangrove regions and the total area of bare surfaces in each of the islands in the years 2010 and 2019 are estimated separately from remote sensing data. From the estimated values, the estimated total throughflow rate is obtained in ml/s. From this, the volume of seasonal throughflow in the Henry's island for each of the seasons are obtained.

Artificial consumption: Consumption of water through all other processes except the physical phenomena described till now is termed here as artificial consumption. This consumption occurs from the local fauna and human activities in the islands.

In the Henry's island, artificial consumption consists of human consumption, consumption by buffaloes, consumption by goats, consumption by ducks and consumption in fisheries. The number of humans present in Henry island varies over the seasons. It is estimated that there are 50 individuals over the pre-monsoon season in Henry island. The daily water consumption by a human is taken as 90 liter, which is equal to $(90/1000) = 0.09$ cubic meter. The number of buffaloes, goats and ducks in Henry island are estimated as 4, 5 and 6, respectively, and these do not vary over the seasons. The volumes of daily water consumption by a buffalo, a goat and a duck are taken as 30 liters, 5 liters and 1 liter, respectively, which are equal to $(30/1000) = 0.03$ cubic meter, $(5/1000) = 0.005$ cubic meters and $(1/1000) = 0.001$ cubic meters, respectively. From the preceding information, the seasonal consumption of water by humans, buffaloes, goats and ducks in the Henry's island is obtained.

The fisheries in the Henry's island consume water in two ways. They consume the rainwater falling into the fish ponds, and each of the ponds undergo water changes once in pre-monsoon and once in post-monsoon. The area and the average depth of a fish pond were measured. There are five fish ponds in Henry islands, and their sizes are taken to be identical. From these information and the rainfall data, the seasonal consumption of water by the fisheries in the Henry's island is estimated.

The seasonal total artificial consumption in the Henry's island is obtained by adding the estimated water consumed by humans, buffaloes, goats and ducks and that consumed by the fisheries.

In the Patibania island, the method of estimating the volume of artificial consumption is

similar with the following differences. There are no buffaloes in the Patibania island, but there are a few cows. The volume of daily water consumption by a cow is taken as 30 liters, which is equal to $(30/1000) = 0.03$ cubic meter. Also, there are no fisheries in the Patibania island, but two ponds are there which consume the rainfall into those ponds. The two ponds are considered having identical sizes, and the surface area and the average depth of a pond were measured. From these measurements and the rainfall data, the seasonal water consumption by the ponds is estimated. The estimated numbers of humans, cows, goats and ducks present in the Patibania island are fixed over the seasons and the years, and the numbers are 2, 2, 3 and 2, respectively. From these numbers and using the same method as followed for the case of the Henry's island, the seasonal water consumption by humans, cows, goats and ducks in the Patibania island is estimated. Finally, the total seasonal artificial consumption of water is estimated by adding the water consumed in the ponds and that consumed by humans and other fauna.

Calculation of water balance: Here, the calculation procedure of the seasonal water balance in the islands is described. Recall that groundwater may be a source of fresh water or may be a consumption point of both freshwater and saline water in a season. For an island, in a particular year and a particular season, the volume of freshwater is obtained by adding the volumes of rainwater and groundwater if groundwater acts as a source of freshwater in that season. Else, the volume of freshwater equals the volume of rainwater in that season. Next, the volume of saline water is estimated by adding the volumes of tidal inundation, tidal prism and cyclone surge in that season. The total inflow of water in the island under consideration in that season is given by the sum of the volumes of freshwater and saline water thus obtained. In the total inflow, the proportions of freshwater and saline water are computed. Next, the total consumption of water in that season is computed by adding the volumes of artificial consumption, surface runoff, channel runoff, throughflow, evaporation and groundwater, in case groundwater acts as a consumption point in that season. Among these, the sum of the volumes of surface runoff, channel runoff, throughflow, evaporation and groundwater, in case groundwater acts as a consumption point, gives the volume of total natural consumption in that season. Now, the volume of water remaining is obtained by subtracting the total volume of consumption from the volume of total inflow of water. From this total volume of water remaining, the volumes of remaining freshwater and remaining saline water are obtained by multiplying the total volume by their respective proportions in the total water inflow.